Recent Advances in Wearable Sensors and Data Analytics for Continuous Monitoring and Analysis of Biomarkers and Symptoms Related to COVID-19

Huijie Li[1†], Jianhe Yuan[2†], Gavin Fennell[1†], Vagif Abdulla[1†], Ravi Nistala[3], Dima Dandachi[4], Dominic K. C. Ho[2]*, Yi Zhang[1]*

[1]Department of Biomedical Engineering and the Institute of Materials Science, University of Connecticut, Storrs, CT 06269, USA.

[2]Department of Electrical Engineering and Computer Science, University of Missouri-Columbia, Columbia, MO 65211, USA

[3]Division of Nephrology, Department of Medicine, University of Missouri-Columbia, Columbia, MO 65212, USA

[4]Division of Infectious Diseases, Department of Medicine, University of Missouri-Columbia, 1 Hospital Drive, Columbia, MO 65212, USA

[†]These authors contribute equally.

[*] Corresponding authors. Email: yi.5.zhang@uconn.edu; hod@missouri.edu

Keywords: wearable sensors, COVID-19, biophysical sensing, biochemical sensing, data analytics, machine learning

Abstract

The COVID-19 pandemic has changed the lives of many people around the world. Based on the available data and published reports, most people diagnosed with COVID-19 exhibit no or mild symptoms and could be discharged home for self-isolation. About 20% of them will progress to a severe disease requiring hospitalization and medical management, including respiratory and circulatory support in the form of supplemental oxygen therapy, mechanical ventilation, vasopressors, etc. The continuous monitoring of patient conditions at home for patients with COVID-19 will allow early determination of disease severity and medical intervention to reduce morbidity and mortality. In addition, this will allow early and safe hospital discharge and free hospital beds for patients who are in need of admission. In this review, we focus on the recent developments in next-generation wearable sensors capable of continuous monitoring of disease symptoms, particularly those associated with COVID-19. These include wearable non/minimally invasive biophysical (temperature, respiratory rate, oxygen saturation, heart rate, and heart rate variability) and biochemical (cytokines, cortisol, and electrolytes) sensors, sensor data analytics, and machine learning-enabled early detection and medical intervention techniques. Together, we aim to inspire the future development of wearable sensors integrated with data analytics that serve as a foundation for disease diagnostics, health monitoring and predictions, and medical interventions.

1. Introduction

The World Health Organization (WHO) has reported cumulatively over 765 million cases and 6.9 million deaths worldwide due to COVID-19 as of May 2023. Due to the limited medical resources, most people diagnosed with COVID-19 are asked to stay home for self-isolation. Multiple studies,

however, have shown that 20% of COVID-19 patients will progress to severe COVID disease, requiring hospitalization and immediate medical intervention.[1] Patients who are required to self-isolate at home might face anxiety for not being properly monitored and treated. Medical grade equipments used in hospitals for such purposes are large, expensive, and require professional staff to operate. Although portable alternatives to some of these systems (typically provided by local health departments in low quantities) exist, they are generally obtrusive and require partial or complete immobilization of the patient in order to achieve reliable continuous monitoring. Furthermore, patients in certain low- and middle-income parts of the world have extremely limited access to health care and/or the ability to afford such technologies, making the matter a global issue.

Wearable sensors that are capable of continuously monitoring a wide range of biomarkers of human physiology, including biophysical and biochemical signals, are promising for unobtrusive, pain-free, accessible, and low-cost assessment at home.[2] Wearable sensors have several key advantages over their non-wearable, traditional counterparts. Firstly, they present unique opportunities for non/minimally invasive monitoring of the vital signs and disease symptoms of interest without the need of the immobilization of the patient.[3, 4] As we will discuss in the following sections, traditional non-wearable technologies used for the acquisition of such information typically involve invasive schemes that induce discomforts for the patient and/or require partial or full immobilization of the patient due to poor interfacing capabilities with the human body. Secondly, the lack of robust interfacing with the human body and the outdated sensing concepts involved deem many traditional technologies unsuitable for continuous monitoring. More specifically, they only provide discrete data points with large, varying time intervals and commonly require manual labor by the patient or a healthcare professional (e.g., thermometers for temperature, blood specimen collection for biochemical analysis, etc.). This is because the interfacing methods of such tools are often obtrusive, uncomfortable, inconsistent and, thus, highly prone to environmental noise, motion artifacts, user error, etc. for long-term continuous measurements. Wearable sensors, on the other hand, are capable of providing robust, consistent, targeted interfaces that overcome many of the above shortcomings and allow for continuous monitoring.[5, 6] Finally, wearable sensors can serve as unique platforms for incorporating novel, ultra-high performance alternative sensing techniques (especially within the context of biochemical sensing) that would not be feasible with traditional technologies.[3, 7] Additionally, wearable sensors can be integrated into common daily items such as smartwatches, fitness trackers, rings, eyeglasses, and more recently, skin patches, bandages, even face masks, contact lenses, and dental devices.[7, 8]

There have been significant advances in the development of wearable biophysical and biochemical sensors over the past few years.[8-12] Here, we report a comprehensive review of the recent progress in wearable biophysical and biochemical sensors capable of monitoring vital signs and symptoms that were found by researchers to have potential significance within the context of the COVID-19 pandemic. Furthermore, we give particular emphasis to flexible, skin-interfaced technologies, which we consider to be "next-generation". The publications preceding the work presented herein have mostly focused on either wearable biophysical[13-18] or biochemical sensors,[7, 19] but not both. Although we acknowledge that both fields are independently very vast and have experienced significant developments in the past few years, we also believe that both are equally relevant within the context of disease diagnosis, monitoring, treatment and, together, they have the potential to

advance personalized healthcare greatly. We summarize and relate the state-of-the-art developments in both fields by giving particular emphasis to disease symptom monitoring, whose importance is strongly highlighted with the ongoing COVID-19 pandemic. Importantly, we present and outline a significant body of research relating the biomarkers and symptoms of interest to COVID-19. Furthermore, we believe that understanding the sensing mechanisms is crucial for inspiring the future research and development of wearable sensors, and potentially for inventing and exploiting novel sensing techniques. Thus, we include these concepts and go into great detail in each section of this review to explain the relevant sensing mechanisms and the physics involved. Moreover, we discuss the more recent, niche sensing technologies and use cases that are promising for the advancement of future wearable sensors. Finally, unlike most publications preceding it, in this work we aim to construct a more complete picture of the field by dedicating a section that focuses on recently emerging data analytics and machine learning methods for data-driven disease diagnostics and medical intervention, with particular emphasis on COVID-19. We believe that these data analytics and machine learning methods, if exploited in conjunction with the next-generation state-of-the-art wearable biophysical and biochemical sensors hereby reviewed, have the potential to allow researchers to design end-to-end systems for personalized remote health monitoring and diagnostics at home.

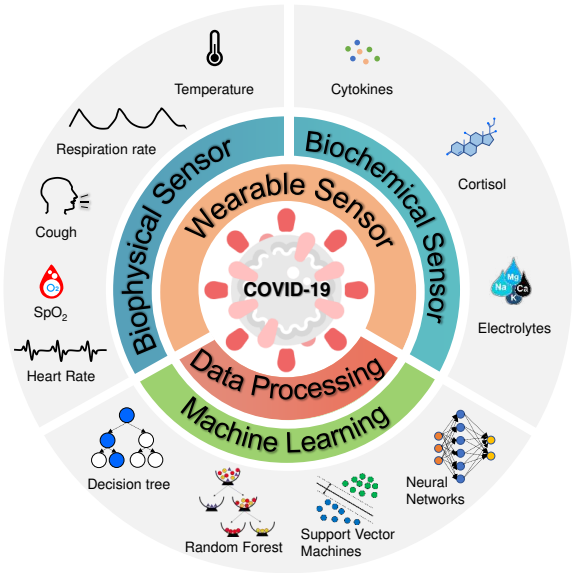

Figure 1. Wearable sensors and data analytics for continuous monitoring and analysis of biomarkers and symptoms related to COVID-19.

The symptoms of COVID-19 patient can range from mild to severe, with possible signs and symptoms including fever, cough, shortness of breath, sore throat, and diarrhea.[20] Although COVID-19 primarily affects the respiratory system, it can also cause health problems in other parts of the body. For example, it may trigger an overreaction of the immune system, known as a

cytokine storm. The purpose of this review paper is to provide an overview of recent developments in wearable sensor technology and data analytics that enable the monitoring and analysis of COVID-19 symptoms. The review is structured as follows (**Figure 1**). The first section focuses on wearable sensing of conventional biophysical information, including body temperature, respiration rate, blood oxygen saturation, heart rate, and heart rate variability. The second section mainly focuses on wearable biochemical sensing, a rapidly emerging field that promises to revolutionize personalized health care through molecular-level monitoring of dynamic metabolic processes and biochemistry content such as cytokines, cortisol, and electrolytes. The final major section of this review focuses on recently developed data analytics and machine learning methods that exploit the vital signs, biomarkers, and symptoms of interest for early detection of COVID-19 and medical intervention.

2. Biophysical sensing for symptoms related to COVID-19

Physical vital signs are critical to monitor as they are indicators of the body's overall homeostasis, and they can serve as a warning system when the body is in the early stages of an infection. In this section, we review the recent developments in wearable biophysical monitoring of disease symptoms, especially those commonly observed in COVID-19 patients, including changes in body temperature, respiration rate, oxygen saturation (SpO_2), heart rate (HR), and heart rate variability (HRV). **Table 1** summarizes the biosensor types, sensing mechanisms and sensing sites of the biophysical sensors for monitoring symptoms of COVID-19.

2.1 Body temperature monitoring

Body temperature is one of human physiology's most important vital signs because its stability is crucial for maintaining the body's homeostasis. Body temperature allows physicians to diagnose and treat infections earlier, rather than waiting for recognizable symptoms to occur. This is because fever is one of the body's first reactions to infectious diseases such as COVID-19. For instance, the maximum body temperature that a patient experiences over the course of their COVID-19 infection was found to be a strong indicator of fatality/mortality.[21] Therefore, measuring body temperature accurately and continuously is of particular importance. Despite its importance, conventional techniques involving thermometers have very limited capability in continuous measurement of body temperature. On the other hand, the gold standards for core body temperature measurement, such as a rectal thermometer or a temperature probe in the esophagus, pulmonary artery, or urinary bladder, are all invasive.[22, 23] Pulmonary artery catheters are only used for critical care and cardiac surgery patients, while rectal thermometers are rarely used due to their invasiveness. Therefore, it is essential to develop temperature sensors that are wearable, noninvasive, easy-to-use, and capable of continuous and accurate monitoring of body temperature.

Within the context of wearable sensors, the temperature can be measured by using the following main types of temperature sensors: negative temperature coefficient (NTC) and positive temperature coefficient (PTC) thermistors and resistance temperature detectors (RTDs). The resistance of NTC thermistors is high at low temperatures due to the lack of free charge carriers. As the temperature increases, thermal agitation causes more free charge carriers (electrons or holes) from the valence band, thereby decreasing the resistance (**Figure 2A**). Unlike NTC thermistors, PTC thermistors have low resistances due to their high dielectric constants below the Curie

temperature, which prevents barriers from forming between the crystal grains. Once the temperature increases above the Curie temperature, the dielectric constant drops. This allows electron-trapping species such as metal vacancies, adsorbed gases, and electron acceptor species to form at the grain boundaries, which causes a dramatic increase in resistance (**Figure 2B**). Similar to PTC thermistors, RTDs, typically made of conducting metals (gold and platinum), have positive temperature coefficients. RTDs take advantage of the temperature coefficient of resistance (TCR) of metals (**Figure 2C**), which is the calculation of the resistance change due to the increase in temperature, given as:

$$R = R_{ref}[1 + \alpha(T - T_{ref})],$$

where α is the temperature coefficient of resistance for conductor material with R and R_{ref} denoting the resistance at test temperature and the reference temperature of the sensor, respectively.

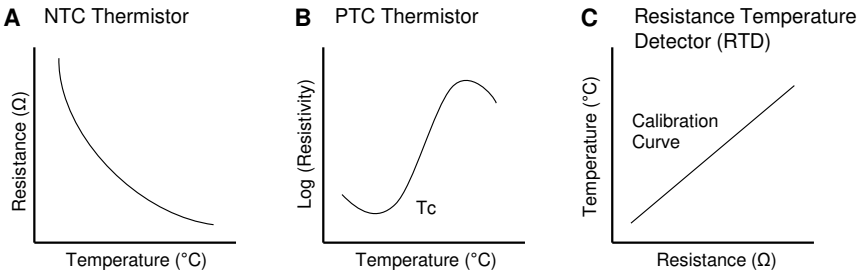

Figure 2. Different types of temperature sensors. (**A**) Resistance change as temperature increases for an NTC thermistor. (**B**) Log (Resistivity) as temperature increases for a PTC thermistor. (**C**) TCR graph for an RTD.

Although they are not widely used in flexible, skin-interfaced wearable sensors, thermocouples are another important type of temperature sensors. Thermocouples are made from two dissimilar electrical conductors (alloys) which form two junctions at different temperatures; a cold junction that acts as a reference and a hot junction where the measurement occurs. The electrical output voltage produced at this junction due to the thermoelectric effect is proportional to the temperature change. This type of temperature sensor can typically operate at much higher temperatures than that of thermistors and RTDs. It also has a much wider working range (-270 °C to 1260 °C). Nevertheless, the low sensitivity associated with thermocouples limits their usage in wearable temperature sensing applications.

Recent advancements in material science, device fabrication technologies, and system integration have enabled the integration of temperature sensors such as NTC and PTC thermistors and RTDs into wearable platforms for continuous body temperature monitoring.[24, 25] For example, Sang et al. developed an ultrasensitive temperature sensor in which a gold-doped silicon nanomembrane array was laminated onto an ultrathin polymer layer in a serpentine mesh structure (**Figure 3A**).[24] Controlling the concentration of Au impurities doped into the silicon nanomembrane results in the

freeze-out region to move closer to the intrinsic region, the shift of Fermi energy level, and the increase the activation energy of p-type silicon nanomembranes. These combined effects increase the device's sensitivity substantially; the sensitivity of the reported sensor is 22 times higher than that of the temperature sensors based on pure gold. For this type of temperature sensor, the concentration of free-electrons increases when the temperature increases due to the formation of electron-hole pairs, which decreases the resistivity of the Au-doped silicon. Importantly, the ultrathin polymer supporting layer allows the sensor to attach conformally to the skin, enabling it to be used with minimal interference from relative movement or sweat during physical activity. The sensor was used to measure an individual's temperature on a stationary bike by placing it on the back and simultaneously monitoring the person's respiration rate by tracking the changes in temperature right below the nostrils when the sensor was attached to the philtrum (**Figure 3B, C**).

It should be noted that the abovementioned temperature sensors measure the skin temperature, not the core body temperature. The measurement of core body temperature is a more accurate representation of human homeostasis, as opposed to the peripheral body temperature, which is generally lower than the core temperature.[26] The gold standard methods (e.g., rectal thermometers, pulmonary artery catheters, etc.) used for measuring core temperature are highly invasive, which makes the use of wearable sensors for estimating the core temperature very appealing. To meet this clinical need, Jeong et al. developed a wireless, multimodal, fully wearable cardiopulmonary monitoring device, which incorporates two temperature sensors to estimate the core body temperature (**Figure 3D**).[27] The two sensors simultaneously measure the skin temperature and the ambient temperature. The skin sensor is located next to the skin in the device and isolated from the ambient sensor using a thermal insulator film to prevent interference from the ambient temperature (**Figure 3E**). The ambient sensor is placed on top of the battery, as far from the skin as possible. It also has a layer of thermal insulator film underneath to isolate it and prevent the battery from influencing the temperature measurements. The advantage of measuring both the skin and ambient temperature is that it allows the device to estimate the core body temperature using a subject-specific model (**Figure 3F**). The device is fully wearable, enabling it to monitor body temperature over long periods while the user is active and transmit the measured data over Bluetooth to be displayed on a user interface. The device was tested on a COVID-19 patient for 171 hours over 8 days during their recovery and was able to continuously monitor the core body temperature, which was observed to decrease from 37.5 °C to 37 °C by the end of the 8 days. The device was also able to monitor the respiration rate, heart rate, cough count, and activity level during that time period.

Wearable temperature sensors could dramatically improve people's ability to monitor body temperature reliably and continuously, thereby enabling the early determination of fluctuations in temperature, either an increase that could imply the progression of an infection or a decrease that could point toward the patient recovering from their disease or infection. Additionally, significant changes in body temperature caused by critical conditions such as hypothermia and hyperthermia can potentially be monitored and detected by wearable continuous body temperature sensors, thereby allowing for better medical intervention. Future improvements need to focus on the removal of motion artifacts which is one of the main shortcomings that many wearable devices suffer from. Creating devices that can conformally attach to the skin helps remove motion artifacts

that are caused by the lack of sufficient and secure contact on the skin during movement.[28] Carefully choosing where to attach the sensor on the body can also help minimize the amount of motion artifacts.[27] Another method of mitigating the influence of daily motion on sensor signal measurements is to perform post-sensor data processing. Band pass filters can be used to remove motion artifacts as long as the relative frequency of those artifacts is known.[29] Signal processing algorithms such as regression, adaptive filtering, blind-source separation, single-source separation, and machine learning can also be used to remove motion artifacts.[30]

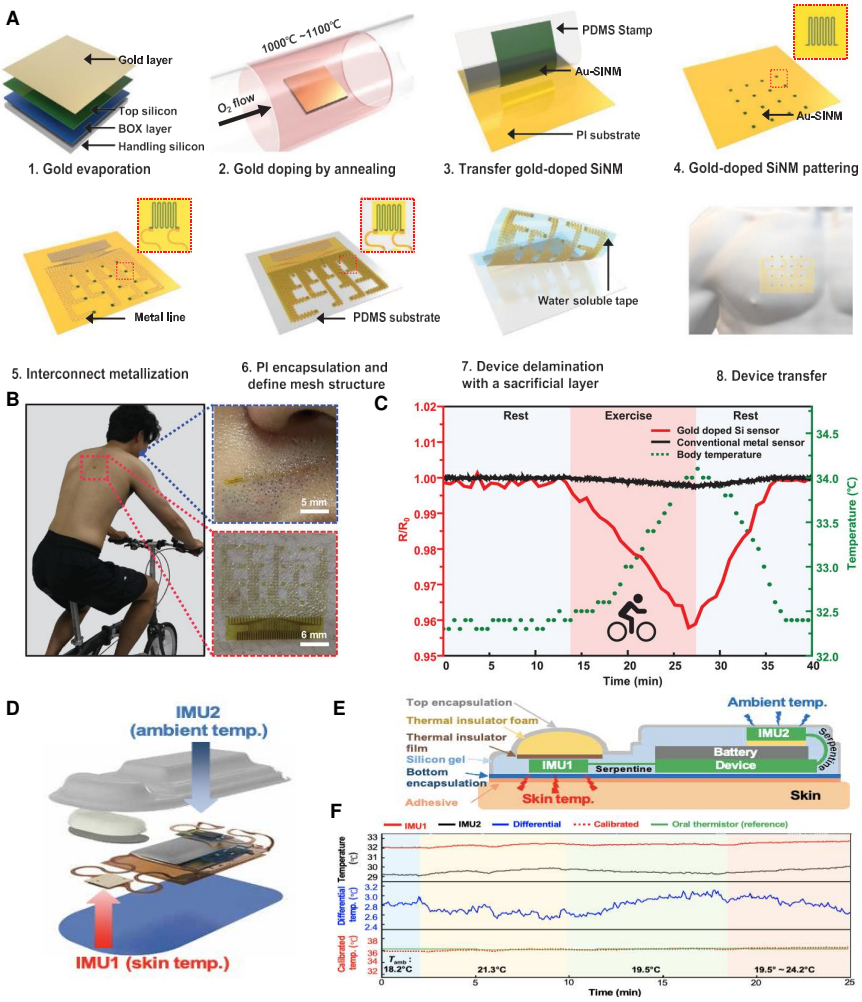

Figure 3. Wearable temperature sensors. (**A**) Schematic illustration for the preparation of a gold-doped silicon nanomembrane epidermal sensor array. (**B**) Photographic images of temperature sensors attached to the skin below the nose and on the back. (**C**) The fractional resistance changes of gold-doped silicon sensors and conventional metal sensors over time during periods of rest and exercise. [(A)-(C)] Figure adopted from Ref 24. Reproduced with permission from M. Sang *et al.,* Adv. Mater. 34 (4), 2105865 (2022). Copyright 2021 Authors, licensed under a Creative Commons Attribution (CC BY) license. (**D**) Schematic illustration of the wearable sensors for core body temperature estimation. (**E**) Labeled Cross-section schematic illustration of the device. (**F**) Comparison of estimated and measured core body temperatures under various ambient temperatures. [(D)-(F)] Figure adopted from Ref 27. Reproduced with permission from H. Jeong *et al.,* Sci. Adv. **7** (20), eabg3092 (2021). Copyright 2021 Authors, licensed under a Creative Commons Attribution (CC BY) license.

2.2 Respiration rate monitoring

Respiratory rate is one of the common vital signs that are frequently assessed in clinical settings. Continuous measurement of respiratory rate is critical for respiratory diseases that cause lung infections, such as COVID-19. Changes in the respiratory rate can accurately predict COVID-19 infections before major symptoms appear.[31-33] The respiratory rate has also been shown to be a good indicator of mortality risk. Chatterjee et al. found that patients with tachypnea (i.e., having respiratory rates of >22 breaths per minute) were at 1.9-to-3.2-fold elevated mortality risk, with 98% of tachypneic patients requiring supplemental oxygen administration.[34] The gold standard for respiration rate monitoring is spirometry, which utilizes a bulky system involving a tube for the patient to breathe into through their mouth. The importance of accurate and continuous respiratory rate monitoring has led to the development of next-generation wearable sensors using alternative sensing techniques. These sensing methods include those based on temperature, humidity, strain, ultrasound, and acceleration.[27, 29, 35-45] The method of interfacing with the body also varies across these modalities.

2.2.1 Thermal sensors for respiration rate monitoring

For instance, temperature and humidity sensors can be placed on the upper lip below the nostrils to track the temperature changes caused by inhaling and exhaling air. The temperature change associated with the inspiration and expiration of air causes the resistance of the integrated temperature sensor to change. By monitoring the resistance change, the respiration rate can be calculated. Liu et al. developed a highly sensitive thermal sensor that can be used to monitor respiration rate when placed on the upper lip beneath the nostrils (**Figures 4A** and **B**).[35] The device consists of a thermal actuator with a fractal curve design made from gold serpentine traces and a miniaturized NTC thermistor. The thermal actuator distributes the heat around the thermistor to increase the temperature difference between the thermistor and exhaled air, enhancing the sensitivity substantially. The temperature changes caused by inhaling and exhaling through the nose cause the resistance of the NTC thermistor to change dramatically allowing the sensor to monitor the respiration rate of the subject. Polydimethylsiloxane (PDMS) is used as a flexible and stretchable base substrate to increase the sensor's conformability. This temperature sensor can monitor respiration rate during exercise and while resting (**Figure 4C**) and distinguish between

PLEASE CITE THIS ARTICLE AS DOI: 10.1063/5.0140900

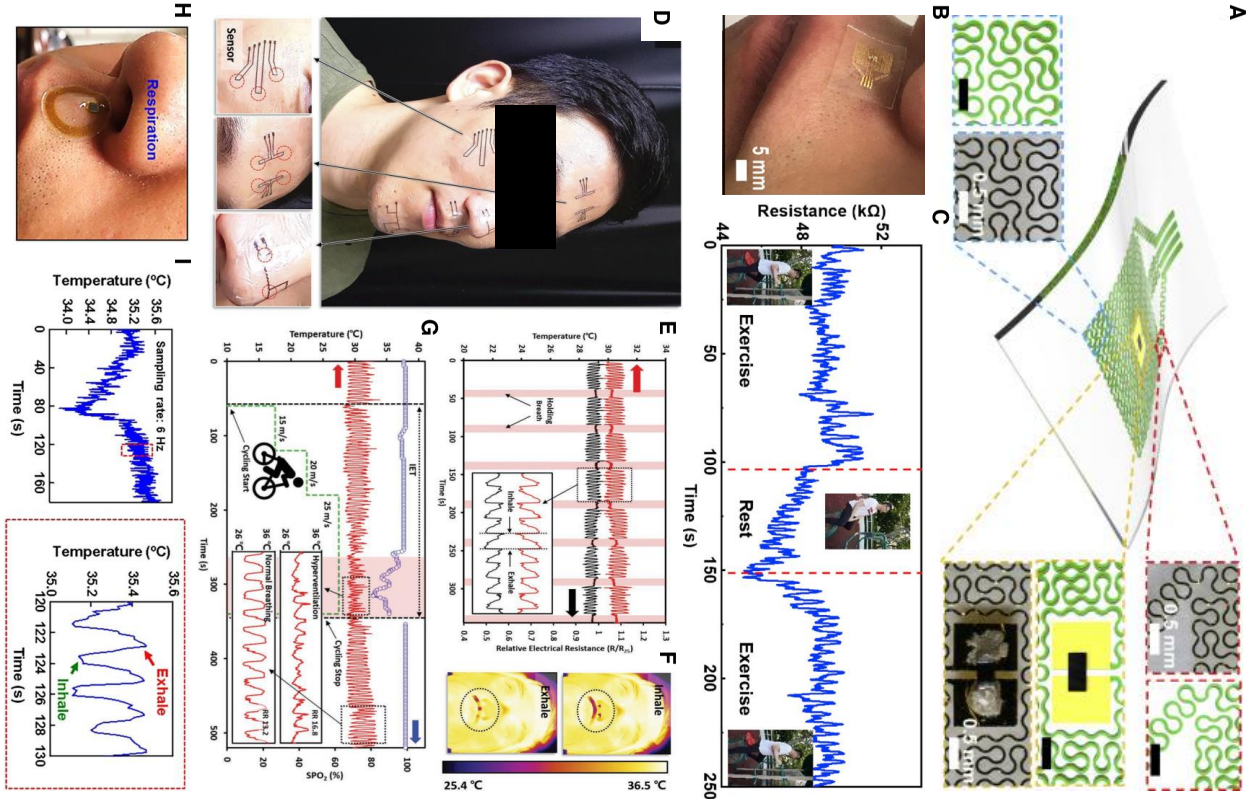

Figure 4. Wearable thermal sensors for respiratory rate monitoring. (**A**) Schematic illustration and optical images of key components of the wearable respiration sensor. (**B**) A photographic image of the assembled respiration monitoring device adhered to the skin beneath the nostrils. (**C**) Resistance changes over time during periods of exercise and rest. Insets show photographic images of the subject exercising and resting. [(A)-(C)] Figure adopted from Ref 35. Reproduced with permission from Y. Liu *et al.,* Mater. Today Phys. **13**, 100199 (2020). Copyright 2020 Elsevier. (**D**) Photographic image of the temperature sensing devices adhered to the skin in different places on the subject's face. (**E**) Temperature changes over time, inset shows zoomed in section of the graph. (**F**) Thermal images of the subject's face when inhaling and exhaling. (**G**) Temperature over time during periods of exercise and rest. [(D)-(G)] Figure adopted from Ref 42. Reproduced with permission from J. Shin *et al.,* Adv. Mater. **32** (2), 1905527 (2020). Copyright 2019 Authors, licensed under a Creative Commons Attribution (CC BY) license. (**H**) Photographic image of respiration monitoring device adhered to the skin beneath the nostrils. (**I**) Temperature over time, inset is zoomed in section of the graph. [(H)-(I)] Figure adopted from Ref 43. Reproduced with permission from S. Han *et al.,* Sci. Transl. Med. **10** (435), eaan4950 (2018). Copyright 2018 American Association for the Advancement of Science.

five different respiratory patterns including gasps, frightened breathing, meditation, sitting, and sleeping. Another temperature sensor that could be placed below the nose to monitor respiration rate was reported by Shin et al. (**Figure 4D**).[42] They made an NTC thermistor-based artificial skin out of an Ni electrode and NiO nanoparticle ink that was coated onto a polyethylene terephthalate (PET) film and then selectively patterned using a laser. The B-value represents the sensitivity of the thermistor, they calculated theirs to be 7350 K in the range of 25-70 °C which they believe to be the highest sensitivity ever reported for a thermistor-based temperature sensor at the time of this paper being published. Their monolithic laser reductive sintering (m-LRS) NiO temperature sensor also has a rapid response time (>50 ms). They were able to conformally attach the device below the nose, showsing the measurement of small temperature changes from inhalation and exhalation to monitor respiration rate (**Figures 4E** and **F**). The device was also able to monitor real time changes in respiration during physical exercise (**Figure 4G**). It is also able to differentiate between normal breathing and shallow breathing due to shallow breathing causing less of a temperature change. A wireless skin-like temperature sensor with near-field communication (NFC) capabilities was reported by Han et al. allowing the sensors to be placed all over the body for large scale temperature mapping without needing batteries or wires.[43] The temperature sensing is achieved using a resistance temperature detector that is built into the NFC chip. The temperature sensing device was adhered to the skin below the nose and was found to be able to monitor the temperature changes caused by inhaling and exhaling allowing it to wirelessly monitor the respiration rate (**Figures 4H** and **I**).

2.2.2 Strain sensors for respiration rate monitoring

In addition to using temperature to measure respiratory rate, strain sensors can be placed on the throat or abdomen to measure the changes in resistance caused by the deformations of the throat and the abdomen during breathing. Liu et al. developed a strain sensor that will slightly deform with the movements of the throat during respiration causing the resistance of the strain sensor to change enabling it to monitor respiration rate and coughing activity using carbonized linen fabric

deposited with polymer-assisted copper (**Figure 5A, B**).[36] Pristine linen woven fabric was carbonized, then underwent polymer growth, and had copper deposited on it before finally being encapsulated in Ecoflex. This strain sensor is highly flexible and sensitive with an ability to stretch up to 300% and a gauge factor of ~ 3557.6 between 0 and 48% strain. It also displays excellent reliability and durability even after 12000 cycles of being repeatedly stretched to 60% strain and released. The sensor can distinguish between normal breathing, coughing, tachypnea, and tachypnea with a cough with high accuracy (**Figure 5C**). Moving from the throat to the abdomen, Xu et al. developed a multifunctional, wearable, wireless sensor system that incorporates a PDMS and laser-induced graphene strain sensor for respiration rate monitoring (**Figure 5D**).[39] The strain sensor is made of a laser induced graphene (LIG) ribbon in the shape of a sideways U with elongated LIG filaments encapsulated in PDMS. The filaments of LIG were elongated to increase the resistance under stretching. This strain sensor is connected to a wireless system allowing for real-time monitoring of respiration rate. When attached to the abdomen of an adult or child, the strain sensor can deform with the movements of the abdomen caused by respiration, causing a change in resistance which is wirelessly transmitted to a smartphone via Bluetooth and can be used to track the respiration rate (**Figure 5E**).

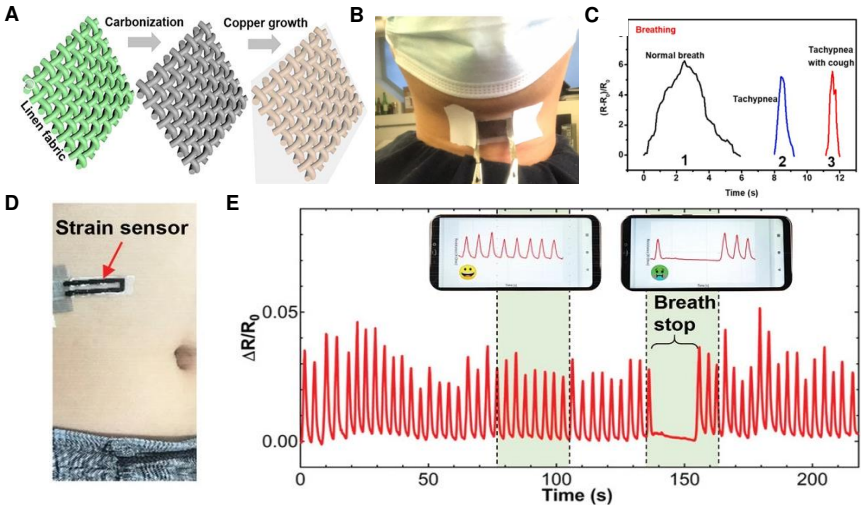

Figure 5. Wearable strain sensors for respiratory rate monitoring. (**A**) Schematic illustration of the carbonized linen fabric strain sensor deposited with polymer-assisted copper (**B**) Photographic image of the strain sensor attached to the throat. (**C**) Relative resistance changes of the strain sensor over time when the wearer is coughing and when the wearer is breathing with or without tachypnea and tachypnea and cough. [(A)-(C)] Figure adopted from Ref 36. Reproduced with permission from Z. Liu *et al.,* Chem. Eng. J. **426**, 130869 (2021). Copyright 2021 Elsevier B.V. (**D**) Photographic image of the LIG strain sensor attached to the abdomen. (**E**) $\Delta R/R_0$ of the strain sensor over time under different conditions. [(D)-(E)] Figure adopted from Ref 39.

Reproduced with permission from K. Xu *et al.,* Adv. Mater. **33** (18), 2008701 (2021). Copyright 2021 Wiley-VCH GmbH.

2.2.3 Mechano-acoustic sensors for respiration rate monitoring

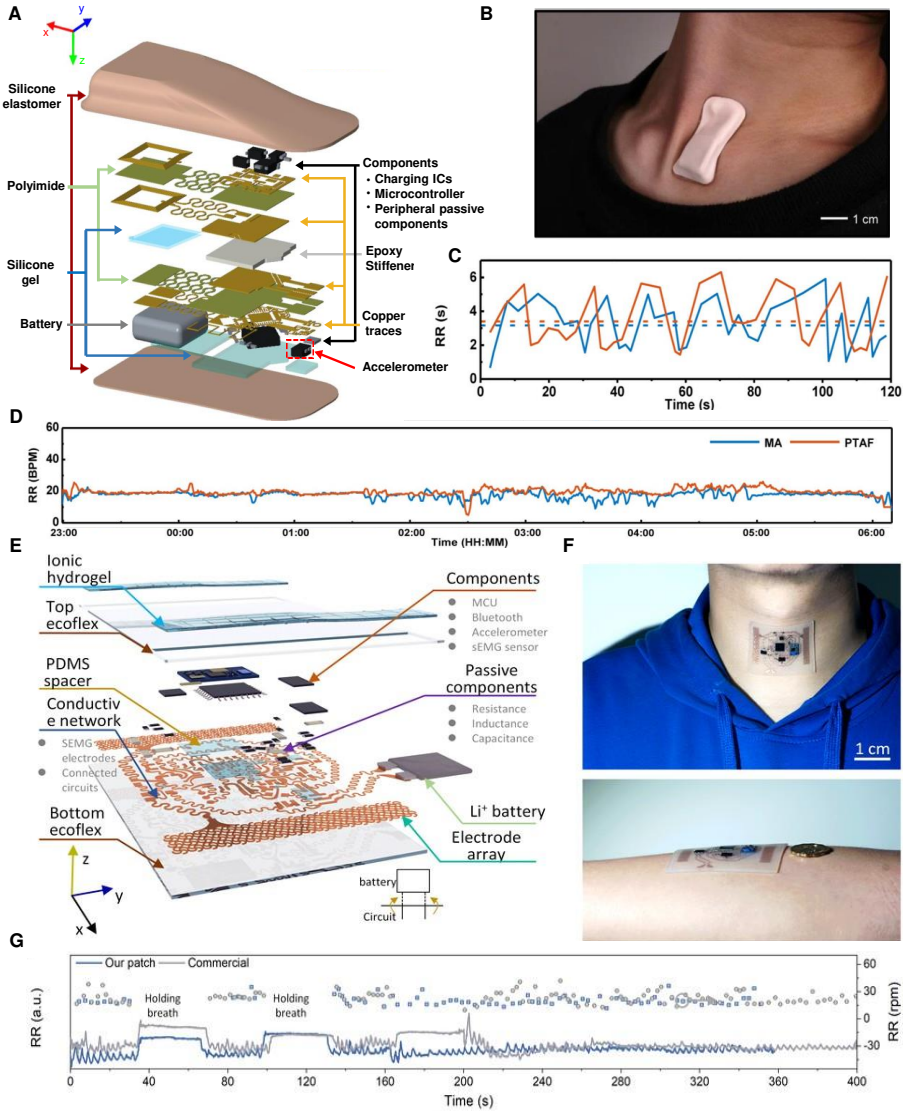

Figure 6. Wearable mechano-acoustic sensor for respiratory rate monitoring. (**A**) Schematic illustration of the exploded view of the mechano-acoustic sensor. (**B**) Photographic image of the device adhered to the suprasternal notch. (**C**) Respiration rate over two minutes using the mechano-acoustic device data and manual counting. (**D**) Respiration rate measured during sleep by the mechano-acoustic sensor and pressure transducer air flow (PTAF) recordings. [(A)-(D)] Figure adopted from Ref 29. Reproduced with permission from K. Lee *et al.,* Nat. Biomed. Eng. **4** (2), 148-158 (2020). Copyright 2019 Springer Nature. (**E**) Schematic illustration of the exploded view of the device system. (**F**) Photographic images of the device adhered to the suprasternal notch of the throat and the arm. (**G**) Comparison of the measured Respiration rate over time of Xu et al.'s device and a commercial device. [44]

Mechano-acoustic sensors can also be used to monitor respiration rate by placing them on the suprasternal notch and using post processing to filter all the acceleration data down to just the data which is caused by respiration. Three-axis digital accelerometers can be placed on the suprasternal notch to measure mechanical motions associated with breathing, enabling respiratory rate estimation. Lee et al. developed a fully wearable wireless system utilizing high bandwidth triaxial accelerometers for mechanoacoustic monitoring of physiologically relevant information such as respiration rate and heart rate (**Figure 6A**).[29] It attaches to the suprasternal notch of the throat and incorporates a rechargeable battery and a Bluetooth chipset into its design for wireless data communication, making it fully wireless and wearable, enabling use during sports, manual labor, or other activities where a wired device could not be used (**Figure 6B**). This device was used to measure respiratory rate while the wearer was awake and asleep (**Figures 6C** and **D**). Breathing produces mechanoacoustic data that accelerometers can track. Specifically, movement of the chest wall during breathing causes a periodic rotation of the device around the y-axis (i.e., yaw) at the neck.[29] Researchers have proposed adding grounded points that do not move with the chest wall to increase the angular range of rotation caused by respiration.[29] Post-data processing using machine learning and frequency-domain analysis take advantage of the time-frequency features to separate the different key events such as respiration rate, heart rate, swallow counts, and energy expenditure. Such platforms were later integrated with sensor data analytics and a cloud data infrastructure to monitor respiratory biomarkers for COVID-19 patients in clinical and home settings.[45] Another mechano-acoustic sensor that can wirelessly monitor vibrations and muscle activity at the suprasternal notch of the throat was reported by Xu et al. (**Figure 6F**).[44] They incorporate an integrated triaxial broad-band accelerometer along with other electronics such as an sEMG onto a thin, stretchable, and flexible Ecoflex substrate to achieve conformal contact with the suprasternal notch and add a composite hydrogel electrode to attain a low contact impedance which improves the signal quality (**Figure 6E**). This sensor utilizes a 2D-like sequential feature extractor with fully connected neurons for data processing which has a high classification accuracy of 98.2% for 13 states/features on five healthy human subjects and can adapt to noisy data. The device platform can also adapt to new subjects with a high classification accuracy of 92%. The weak vibrations of lung dilatation processes can be detected by the accelerometer in this device as acceleration along the y axis which can then be processed using digital filtering and peak-detection allowing this device to monitor respiration rate (**Figure 6G**). Moving from the suprasternal notch to the abdomen, Shahshahani et al. developed a wearable ultrasound-based sensor for diaphragm motion tracking and respiration rate monitoring.[40, 41] It is placed near the abdomen on the zone of

apposition (ZOA) to reduce motion artifacts from the upper body (i.e., the heart, etc.). Their device uses a single PZT5 piezo disk transducer to send ultrasound signals to the diaphragm, from which the echoed signals are then received and measured. The respiration rate is calculated by tracking the position of the organ using the intensity and time of flight (ToF) of reflected sound. When compared against the gold standard (i.e., spirometer), the sensor outperformed the methods using photoplethysmography (PPG) and inertial sensors.

2.3 Blood oxygen saturation, heart rate, and heart rate variability monitoring

Using the skin as a translucent medium, various wearable sensors can be engineered to optically and non-invasively measure certain biomarkers of human physiology. These important biomarkers include SpO_2, HR, and HRV. SpO_2, often described in terms of percentages, is a quantitative measure of the amount of oxygen-saturated hemoglobin with respect to the total hemoglobin in the blood.[46] Following the oxygenation process in the lungs, saturated hemoglobin facilitates the distribution of oxygen throughout the entire body. As a result, blood SpO_2 levels are directly influenced by the respiratory system. The SpO_2 levels of patients with SARS-CoV-2 or other respiratory infections can display values well below the normal range due to the respiratory dysfunctions of varying degrees caused by lung inflammation.[47] Specifically, SpO_2 levels of lower than 92% were shown to an increased likelihood of hospitalization (relative risk = 7.0), as well as elevated risk of intensive care unit (ICU) admission, septic shock, and acute respiratory distress syndrome among 209 suspected patients (77 tested positive for COVID-19). Therefore, continuous and accurate monitoring of SpO_2 is of particular importance for COVID-19 patients.

HR and HRV are two other important biomarkers that are closely related to each other. HR refers to the number of heart beats per minute, whereas HRV describes the variation in the interbeat time intervals and is usually measured in terms of standard deviations in the time domain.[48] In search of more easily acquired biomarkers that can reliably predict the outcomes of COVID-19 disease, HR and HRV have been extensively studied.[49-52] Frequency domain analysis of HRV has revealed that high (HF) and low (LF) frequency powers of the spectrum exhibit a significant reduction in COVID-19 patients, whereas time domain measures such as root mean square of successive R-to-R peak interval differences (rMSSD) and standard deviation of NN intervals (SDNN) showed increased values, indicating elevated parasympathetic activity.[49] Moreover, the increased HRV in COVID-19 patients of age 70 and higher predicted greater odds of survival, while low HRV implied ICU admission in the first week of hospitalization.[50] Another study has revealed that the aforementioned decrease in HRV could be a good predictor of increases in C-reactive protein (CRP), which is now commonly used to track the patient's inflammatory response caused by SARS-CoV-2.[51] Additionally, HR has been shown to exhibit elevated baseline values in fetuses of pregnant COVID-19 patients, presumably due to the effects of the maternal inflammatory response, maternal pyrexia, and cytokine storm.[52] Acquisition of HR and HRV continuously and accurately is, therefore, appealing within the clinical context.

SpO_2, HR, and HRV measurements can all be acquired classically through PPG signals using pulse oximetry, an optical technique that is typically non-invasive.[53] In the case of SpO_2 monitoring, red blood cells saturated with oxygen possess a unique shade of red. This sets the basis for the working principle of a pulse oximeter, which measures the difference in light intensities caused by the unique absorbance characteristics of oxygenated and deoxygenated hemoglobin at different wavelengths.[46, 54] More specifically, oxygenated (deoxygenated) hemoglobin lets more red (infrared) light pass through while absorbing more infrared (red) light (**Figure 7A**). Therefore, a

basic pulse oximeter requires only three components at its core: a red light source operating at ~660 nm (R), an infrared light source operating at ~940 nm (IR), and a photodetector (PD) (**Figure 7B**). Upon the illumination of the tissue through the skin, the PD measures the intensities of either the transmitted (i.e., transmission-based oximetry) or reflected (i.e., reflectance-based oximetry) R and IR light. Then, a processor (i.e., a microcontroller) digitizes the PD voltage signals through an analog-to-digital converter (ADC) and performs a simple calculation to find the light ratio between the two measured wavelengths of light. Finally, this ratio is used to generate a calibration curve using the Beer-Lambert law, from which the SpO_2 level is determined. This method of non-invasively measuring peripheral SpO_2 levels in a controlled clinical environment has been shown to be within 3-4% (2-3% for continuous monitoring) accuracy of the more accurate, invasive arterial SpO_2 measurements.[54] The level of accuracy achieved is considered to be sufficient for most cases; however, more accurate methods may be required for oxygenation monitoring of critically ill patients and newborn infants due to the fact that the calibration curves for pulse oximetry are generally derived from healthy individuals of higher ages. Consequently, non-invasive medical grade pulse oximeters alone generally do not provide decisive readings and hence are often used in combination with other monitoring systems to improve diagnostics in clinical settings, especially for COVID-19 patients.[55]

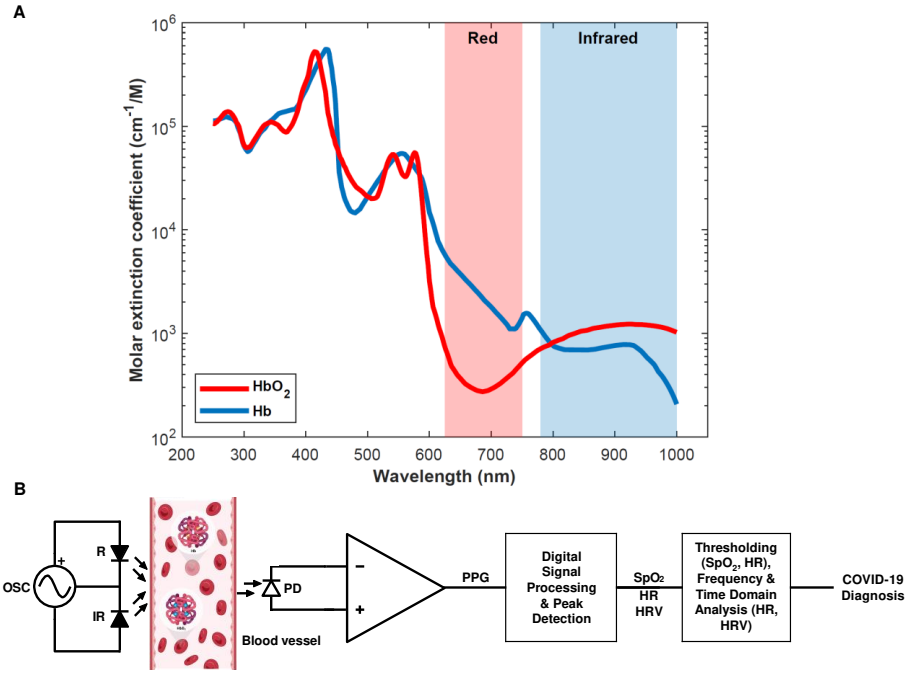

Figure 7. Principles of pulse oximetry-based COVID-19 diagnosis. (**A**) Absorption spectra of oxygenated (HbO_2, red line) and deoxygenated (Hb, blue line) hemoglobin. Reversed differences in absorption levels at red (shaded red) and infrared (shaded blue) wavelengths set the basis for

pulse oximetry. Reproduced from Prahl S. Data available at: https://omlc.org/spectra/hemoglobin/index.html. Accessed May 22, 2022. (**B**) System block diagram of a basic transmission-based pulse oximeter. The PD senses the intensities of reflected or transmitted lights from the tissue (insets are HbO_2 and Hb inside a blood vessel) due to the R and IR LEDs, which are then amplified to generate a photoplethysmogram (PPG). SpO_2, HR, and HRV values are extracted from the PPG signal through digital processing and peak detection algorithms. By analyzing these values through appropriate methods such as thresholding and time/frequency domain techniques, COVID-19 disease assessment and diagnosis can be performed.

Furthermore, since PPG signals display periodic peaks that correspond to cardiac cycles caused by pulsative volumetric changes in the blood vessels, HR and HRV information can be computationally extracted from the PPG signals using appropriate peak detection algorithms.[53] After the SpO_2, HR, and HRV values are collected, they can be further processed using aforementioned methods such as thresholding (i.e., comparing against a fixed or an adaptive value), time (i.e, standard deviation) and frequency (i.e., power spectra) domain analysis to complete a workflow for pulse oximetry-based COVID-19 disease diagnosis (**Figure 7B**).

Despite the widespread popularity of non-invasive pulse oximeters in clinical settings (e.g., fingertip or earlobe-worn medical oximeters) and consumer electronics (e.g., wrist-worn smartwatches and fitness trackers), conventional technologies used in their implementations impose multiple limitations. Since non-invasive pulse oximetry employs optical methods, only a few body areas such as the fingertips and the earlobes (although less common, the forehead can also be targeted) are well suited for performing medical-grade measurements due to their higher translucency.[56] However, clinical pulse oximeters are not suitable for SpO_2 monitoring of moving subjects because of their susceptibility to motion artifacts and bulky, rigid construction. Considering that most people infected with SARS-CoV-2 are not immediately aware of it, continuous and remote SpO_2 monitoring on a daily basis could be crucial for the early detection of the disease. Although wrist-worn sensors in the form of smartwatches or fitness trackers are more convenient for daily usage, and some of them can be utilized for reasonably reliable measurements of HR and HRV,[57, 58] they are generally considered to be not accurate enough for SpO_2 monitoring.[56, 59] While more robust algorithms can be developed to improve the accuracy of SpO_2 readings from the wrist,[60] lack of sufficient contact and extensive motion present around the wrist introduce large baseline errors[61] that are difficult to account for without additional readings from fused sensors such as inertial measurement units (IMUs). Such methods predictably require additional hardware and increase complexity.

The emergence of next-generation skin-interfaced electronic devices that employ soft, flexible, and/or stretchable materials in their construction presents unique opportunities for developing wearable, non-invasive optical sensors whose mechanical properties match those of the epidermis.[62, 63] Such sensors exploit alternative materials and fabrication methodologies for their core electronic components, namely PDs and light-emitting diodes (LEDs).[64-66] These devices achieve conformal contact with the skin to minimize motion artifacts, which greatly improves the accuracy and reliability of the measurements of relevant biomarkers such as SpO_2, HR, and HRV and enable monitoring from a wider range of body locations. This gives PPG the edge over alternative methods such as electrocardiography (ECG) for wearable HR and HRV monitoring. ECG is easily influenced by electromyograph (EMG) signals generated by muscle activation and other electrical noise, which constraints ECG to only chest-based recordings due to the increased

signal-to-noise ratio for daily wearable sensing and for clinical applications involving patients with tremor or hyperkinesia.[14, 67] For these reasons, as well as PPG's similar HR/HRV performance and ability to measure SpO_2, we do not discuss wearable ECG sensors for HR and HRV monitoring in this work (the reader is encouraged to check papers from Chen et al.[16] and Hong et al. [14] for the discussion of wearable ECG sensors). The skin-like properties of epidermal pulse oximeters make them significantly less noticeable to the user, offering new convenient ways for remote monitoring of moving subjects.[13-18, 68] Below, we summarize the recent advances in wearable optical sensors for skin-interfaced pulse oximetry.

Yokota et al. developed a flexible photonic skin using organic materials that can monitor the SpO_2 levels using reflectance-based pulse oximetry.[69] This device can stretch up to 200 %, allowing it to be unobtrusively attached to the fingertip for oximetry measurements. A similar organic flexible sensor patch, described by Lee et al., improves upon the previous sensor by exploiting a unique "8"-shaped geometry to minimize the stray propagation of the emitted light from the LEDs (**Figure 8A**).[70] The sensor reliably operates at ultra-low electrical power levels, enabling all-day PPG and SpO_2 monitoring of the user (**Figure 8B**). Khan et al. developed a flexible organic sensor array to achieve spatial oxygenation mapping capabilities in different body areas beyond the conventional sensing sites.[71] The authors later fabricated a multi-channel pulse oximeter that, when paired with algorithms to take advantage of the redundancy of the measurements, can improve HR detection (**Figures 8C, D**).[72] In order to realize pulse oximetry that is unnoticeable to the user, Kim et al. developed an ultra-miniaturized wireless pulse oximetry system that attaches to the fingernail or the earlobe and utilizes near-field communication (NFC) for power delivery and PPG data transmission.[73] The device is fabricated on a flexible sheet of Cu (18 μm)/polyimide (PI, 12 μm)/Cu (18 μm) foil through photolithography. The electronic components are soldered in and then encapsulated within a soft silicone elastomer. Chung et al. later developed an improved, epidermal version of the previous device using stretchable serpentine Cu electrical traces embedded in an ultra-thin, soft, skin-like elastomer to combine PPG pulse oximetry and ECG for neonatal intensive care with on-device signal processing and high-bandwidth data transmission through Bluetooth (**Figures 8E, F,** and **G**).[74] The following set of recent developments involves introductions of distinctive approaches and novel technologies to advance wearable optical sensing and pulse oximetry forward going into the future.

To this end, a wearable transcutaneous oxygen ($tcpO_2$, measure of oxygen level as opposed to saturation level) sensor was fabricated by Lim et al. using a photoluminescent oxygen-sensing film.[75] This sensor incorporates an indium tin oxide (ITO) thin-film heater layer to increase the local temperature of the target skin area to promote arterialization and, therefore, enhance $tcpO_2$ measurements. Abdollahi et al. followed a unique approach to develop patient-specific pulse oximeters.[76] The sensor is incorporated into a flexible cuff system which is fabricated according to the measurements of the target sensing area (i.e., finger or toe) of a particular patient through advanced PDMS 3D printing. This personalized cuff is then interfaced with the main board for data processing and transmission. In order to greatly enhance the interfacing capabilities and increase the emission area of wearable LEDs, Bae et al. proposed a new approach to fabricate PDMS-based stretchable waveguides.[78] Another major improvement to the existing wearable pulse oximeters was introduced by Han et al., where the authors achieved high-performance pulse oximetry using only ambient light without the use of LEDs by combining organic PDs with spectrally selective filters to achieve sensitivity peaks at near-infrared (~740 nm), red (~610 nm), and green (~525 nm) wavelengths (**Figures 8H, I**).[77] The elimination of the LEDs and reliable

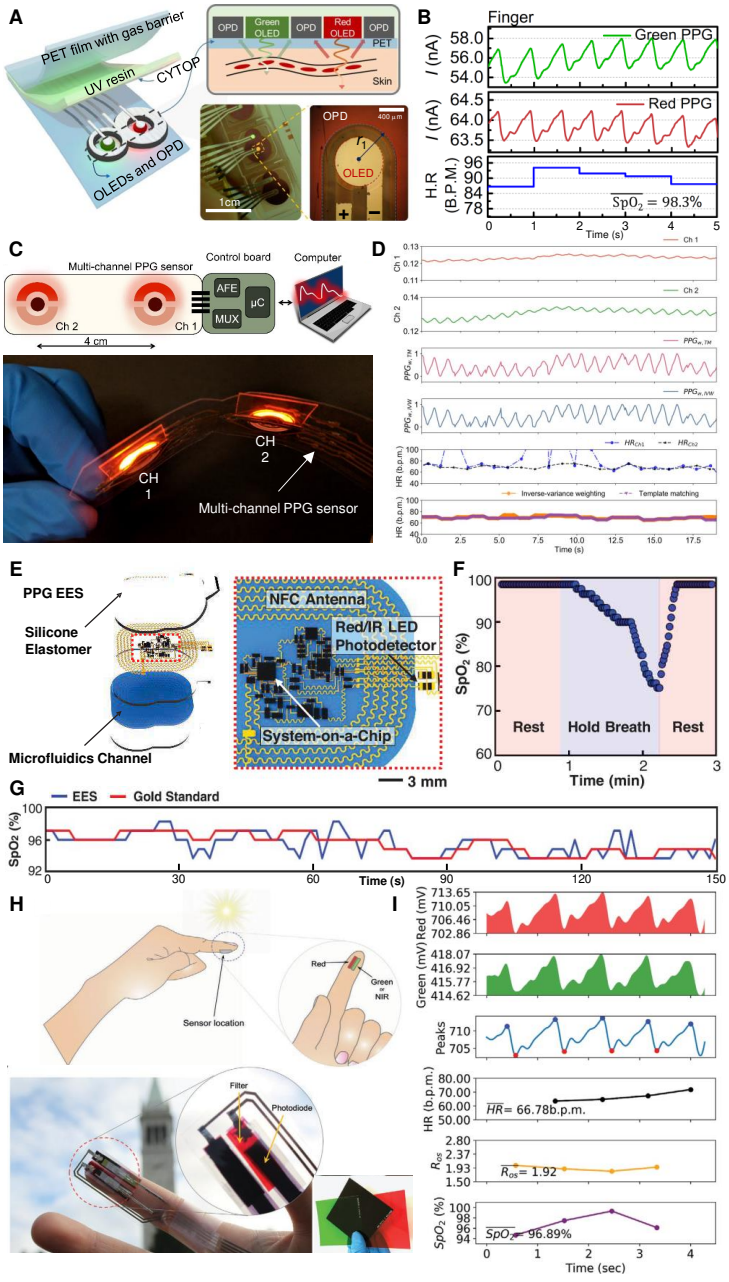

Figure 8. Recent advances in wearable optical sensors for pulse oximetry. (**A**) Schematic illustrations and photographic images of an organic flexible sensor patch optimized for power efficiency. (**B**) PPG measurements using the wearable sensor patch placed on the fingertip and extracted HR/SpO_2 information. [(A)-(B)] Figure adopted from Ref 70. Reproduced with permission from H. Lee *et al.,* Sci. Adv. **4** (11), eaas9530 (2018). Copyright 2018 Authors, licensed under a Creative Commons Attribution (CC BY) license. (**C**) Schematic illustration and photographic image of a flexible multi-channel wearable pulse oximeter. (**D**) Raw (first and second panels) and weight-adjusted (third and fourth panels) PPG measurements from the multi-channel sensor, HR estimations from the two channels (fifth panel), and HR estimations of two multi-channel extraction algorithms (sixth panel). [(C)-(D)] Figure adopted from Ref 72. Reproduced with permission from Y. Khan *et al.,* IEEE Access **7**, 128114-128124 (2019). Copyright 2019 Authors, licensed under a Creative Commons Attribution (CC BY) license. (**E**) Schematic illustration of a wireless, battery-free epidermal electronic system (EES) for PPG measurements in neonatal intensive care. (**F**) Real-time, on-device SpO_2 monitoring using the PPG EES during a breathing exercise. (**G**) SpO_2 monitoring performance of the PPG EES compared to the gold standard system (Intellivue MX800, Philips). [(E)-(G)] Figure adopted from Ref 74. Reproduced with permission from H. U. Chung *et al.,* Science **363** (6430), eaau0780 (2019). Copyright 2019 Authors, licensed under a Creative Commons Attribution (CC BY) license. (**H**) Schematic illustrations and photographic images of a LED-free pulse oximeter that uses ambient light. Insets display the various spectral filters designed to be integrated with the PDs to selectively sense the wavelengths of interest. (**I**) Fingertip pulse oximetry measurements using the sun as a light source with green and red spectral filters. [(H)-(I)] Figure adopted from Ref 77. Reproduced with permission from D. Han *et al.,* Adv. Mater. Technol. **5** (5), 1901122 (2020). Copyright 2020 WILEY-VCH Verlag GmbH & Co. KGaA, Weinheim.

operation in both indoor and outdoor lighting conditions make ambient light oximeters appealing for realizing low-cost and efficient pulse oximetry systems.

An alternative method that can be used to measure blood oxygenation is photoacoustic tomography (PAT), which is a powerful, emerging hybrid method that combines optical stimulation of tissue and ultrasonic transduction[79, 80] PAT has found applications in alternative monitoring of blood oxygenation thanks to its excellent contrast due to targeted optical excitation and deep tissue penetrating capabilities resulting from nature of the ultrasonic signals received.[81, 82] Only recently, PAT has been incorporated into flexible, skin-interfaced wearable sensors by Gao et al. in the form of a photoacoustic patch for 3D imaging of hemoglobin in the blood.[83] The sensor uses microfabricated vertical-cavity surface-emitting laser (VCSEL) diodes on an elastomeric polymer in order to excite the hemoglobin molecules in deep tissue (>2 cm), causing them to emit acoustic ultrasound waves which are then detected by the piezoelectric transducers integrated onto the same sensor patch. Although only total hemoglobin was measured, the sensor patch can easily be modified to incorporate two different VCSEL diode wavelengths in order to distinguish oxygenated hemoglobin from deoxygenated hemoglobin and measure SpO_2, akin to the red and infrared LEDs used in pulse oximetry. Furthermore, exploiting the linear relationship between the amplitude of the photoacoustic response signals with core temperature, the authors were able to generate an accurate 3D map of the core temperature within the imaging field of view.

Table 1. Biophysical sensors for monitoring symptoms of COVID-19.

Biophysical Vital Sign	Type of Biosensor	Sensing Mechanism	Sensing Site	Ref.
Body Temperature	Gold doped silicon nanomembrane array - NTC Thermistor	Electrical resistance decreases as temperature increases	Arbitrary location on the torso	24
	Integrated circuits (ICs) with silicon bandgap temperature sensors	Voltage difference between two silicon p-n junctions increases as temperature increases	Neck area	27
Respiration Rate	Thermal actuator and NTC Thermistor	Electrical resistance decreases as temperature increases	Upper lip	35
	Carbonized linen deposited with copper strain sensor	Electrical resistance changes with deformation	Throat	36
	Laser-induced graphene strain sensor	Electrical resistance changes with deformation	Abdomen	39
	Three-axis digital accelerometers	Periodic rotation of the device due to breathing	Suprasternal notch	29
	Ultrasound PZT5 piezo disk transducer	Ultrasound time of flight changes with the movement of the diaphragm	Abdomen (zone of apposition)	40
Oxygen Saturation (SpO_2), Heart Rate (HR), and Heart Rate Variability (HRV)	Organic/polymer LEDs and organic PDs integrated in optoelectronic skin	Reflectance pulse oximetry	Arbitrary location on the body	70
	Sensor patch with two pairs of organic LEDs and organic PDs for data redundancy	Reflectance pulse oximetry	Wrist	72
	NFC patch fabricated on a flexible sheet of Cu/PI/Cu through photolithography	Reflectance pulse oximetry	Arbitrary location on the torso and limbs	74

	embedded in soft silicone elastomer		(neonatal care)	
	Organic PDs with spectrally selective filters for LED-free pulse oximetry using only ambient light	Transmission pulse oximetry	Index finger	77
	An array of microfabricated VCSEL diodes and piezoelectric transducers embedded in soft silicone elastomer	Photoacoustic tomography	Arbitrary location on the body	83

3. Biochemical Sensors for Symptoms Related to COVID-19

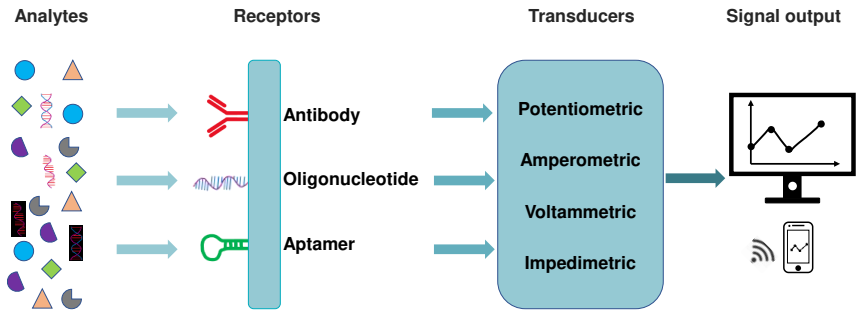

Figure 9. Schematic illustration of the key components of a typical electrochemical biosensor

Wearable biosensors are promising for non-/minimally invasive, continuous, and real-time monitoring of vital physiological information in personalized medicine. Early efforts of wearable sensors focused on monitoring the human body's physical activities, including heart rate,[84] body movement,[85] blood pressure,[86] body temperature,[87] respiration rate,[39] and ECG, etc.[62, 88] However, the development of wearable devices capable of providing direct information on the dynamic biochemical and metabolic processes at the molecular level is still in its infancy.[89] Furthermore, multiplexed biochemical monitoring could detect COVID-19-associated early symptoms and track the progression of illness, thereby enabling a more accurate disease diagnosis and treatment. The current standards of monitoring various biochemicals, including antigens and antibodies, electrolytes, metabolites, and cytokines involve frequent sampling of blood or urine in the laboratory. Such sample collection and testing procedures are painful, time-consuming, and pose a barrier to their usage in the continuous monitoring of biomarkers. In addition, those sampling and testing procedures increase the number of healthcare worker/patient interactions and require additional use of personal protective equipment (PPE). There remains an urgent need for personalized, simple, and effective ways to monitor health status by measuring multiple biochemical markers such as, electrolytes, cytokines, and cortisol, all of which provide critical information for the prediction, screening, diagnosis, and therapy of COVID-19.[90-94]

Typical biochemical sensors consist of three key components; "receptors" (e.g., antibody, oligonucleotide, aptamer, etc.) for selective binding to the target analytes, "transducers" that convert the target-receptor interaction into measurable signals such as electric potential, current, impedance, etc. (**Figure 9**), enabling the sensitive and selective detection of biochemicals, and a readout system that stores, processes, and displays the measurable sensor signals. In this section, we will mainly review the recent development of wearable biochemical sensors for monitoring cytokines, cortisol, and electrolytes for COVID-19 patients (**Table 2**).

Table 2. Biochemical sensors for monitoring symptoms related with COVID-19

Analyte	Type of Biosensor	Type of Transduction	Matrix Analyzed	Limit of detection (LOD)	Ref.
IFN-γ	Graphene field-effect transistor (gFET)-based aptameric sensor	FET	Sweat	7.4×10^{-13} mol L^{-1}	90
IFN-γ, TNF-α, and IL-6	Graphene field-effect transistor (gFET)-based aptameric sensor	FET	Serum Saliva Urine Sweat	4.75×10^{-13} mol L^{-1} 6.08×10^{-13} mol L^{-1} 6.11×10^{-13} mol L^{-1}	91
Cortisol	Molecularly imprinted polymer-based organic electrochemical transistors (OECTs)	OECTs	Sweat	3.8×10^{-7} mol L^{-1}	103
	Antibody-electrochemical sensor	Amperometric	Sweat Saliva	2.21×10^{-10} mol L^{-1}	104
	Aptamer-field-effect transistor	FET	Sweat	1×10^{-12} mol L^{-1}	105
Na^+, K^+	Electrochemical-potentiometric	Sodium and potassium ISE	Interstitial fluids	-	106
Na^+	Graphene field-effect transistor	Ion-sensitive field-effect transistor (ISFET)	Interstitial fluids	2.78×10^{-6} mol L^{-1}	94

3.1 Cytokine monitoring

SARS-CoV-2 infections can cause excessive levels of hyper-inflammatory cytokine in the serum, which is known as the cytokine storm.[95] Some studies suggest that the cytokine storm is a possible cause of death for COVID-19 patients and that the level of cytokine can be used as an effective predictor for disease severity, progression, and recovery.[96] Recently, interleukin-6 (IL-6) and interferon-alpha (IFN-α) were reported to be positively correlated with severe cases. For instance, IL-6 is associated with hospitalization, ICU admission, and poor prognosis.[97-101] High serum IFN-α level was found in severe cases during COVID-19.[98] Therefore, before prescribing immunosuppressive therapy, the cytokine panel should be evaluated to precisely identify the needs of each patient.[102]

Figure 10. Wearable cytokine sensors. (**A**) Schematic illustration of the graphene-Nafion film based regenerative sensor for cytokine detection. Figure adopted from Ref 90. Reproduced with permission from Z. Wang *et al.,* Adv. Funct. Mater. 31 (4), 2005958 (2021). Copyright 2020 Wiley-VCH GmbH. (**B**) Illustration of aptameric dual channel graphene-based biosensing system for multiplex detection of IFN-γ, TNF-α, and IL-6 in cytokine storm caused by SARS-CoV-2. Figure adopted from Ref 91. Reproduced with permission from Z. Hao *et al.,* Small 17 (29), 2101508 (2021). Copyright 2021 Wiley-VCH GmbH.

Protein biomarkers, like cytokines, are typically detected by immunosensors in which antibodies are used as sensor receptors. As the receptors, antibodies can specifically recognize targets. However, their practical applications are still limited by their large molecular size, limited lifetime, temperature sensitivity, susceptible to contaminated, irreversible denaturation,[96] and complicated operations, which will be difficult in wearable sensor applications. Different from the antibodies generated from animals through complex processes, aptamers are chemically synthesized with lower prices, higher stability, longer shelf life, and lower variation from batch-to-batch. More importantly, it is much easier to induce chemical modification at any desired location in the chain of nucleotides.[107] For example, by using the specific aptamer of the target, Wang et al. reported a flexible and regenerative graphene field-effect transistor (gFET)-based aptameric sensor for interferon-gamma (IFN-γ) detection down to 740 fM in undiluted human sweat (**Figure 10A**).[90] Specifically, by drop-casting Nafion solution onto the graphene surface to form a Nafion film, graphene was isolated with the nontarget molecules to minimize the nonspecific adsorption of graphene, allowing the regeneration and reuse of the gFET by dissolving the Nafion film in ethanol. Moreover, this device demonstrated excellent electrical and mechanical performance, with no obvious mechanical damage and maintained a consistent electrical response over up to 80 cycles of regeneration and up to 100 cycles of crumpling tests, respectively. Additionally, by exploiting the flexibility and durability of the graphene-Nafion composite film, this sensor exhibited conformal attachment to human skin under deformation, implying the potential for wearable applications. Different from techniques for single biomarker detection, a sensing system that enables simultaneous detection of multiple cytokines could provide more information for disease screening, diagnosis, and therapy, which is especially important for early identification of the COVID-19 infection for asymptomatic and presymptomatic individuals. Recently, Hao et al. [91] developed an aptameric dual-channel graphene-based biosensing system for multiplexed detection of IFN-γ, TNF-α, and IL-6 in human biofluids, including serum, saliva, urine, and sweat within 7 min with detection limits as low as 475 fM, 608 fM, 611 fM, respectively (**Figure 10B**). This

multi-sensing system integrates a customized device for signal processing, display, and wireless data transmission to a smart device and notifies the individuals when their physical condition gets worse. Additionally, this intelligent graphene-based biosensing device demonstrated satisfactory performance for wearable applications in COVID-19 patients when the sensor was fabricated on a flexible polyethylene terephthalate (PET) substrate for cytokine detection in sweat.

3.2 Cortisol monitoring

Cortisol is generated by the human body in response to stress. Abnormally high or low cortisol concentrations can be life-threatening.[93] In particular, excessive levels of cortisol can aggravate a patient's condition, leading to a weaker immune system and a higher risk of infection. A new study led by Dr. Dhillo et al. found that COVID-19 patients with high concentrations of total cortisol in their serum are more likely to have their condition deteriorate quickly, leading to death.[93] Thus, cortisol levels can be a key biomarker to indicate the severity of COVID-19 infection and can be used as valuable information for medical personnel to identify COVID-19 patients who may need intensive care. Parlak and co-workers developed a wearable organic electrochemical transistor (OECT) for continuous non-invasive monitoring of cortisol in sweat.[103] This sensor system consists of multifunctional layers, including microcapillary channel arrays for sweat sampling, molecularly imprinted polymer (MIP)-coated organic electrochemical transistors that can selectively bind with cortisol, and a water-proof protection layer (**Figure 11A**). **Figure 11B** shows the analytical performance of the developed sensor for on-body measurement by spraying artificial sweat with various cortisol concentrations on the forearm, including the sensor output current response as a function of cortisol concentration and the corresponding calibration curve. The developed sensor was also tested with real sweat from the skin, showing a strong correlation with standard ELISA methods (**Figure 11B**). With microfluidics technology, sweat can be rapidly sampled by the laser-patterned channel arrays from the skin surface without sensor contamination. The sensing principle involves the binding of the MIP and target, resulting in the sealing and blocking of the membrane pores, which prevents ion transport to the channel. This allows for the detection of cortisol concentration by measuring changes in source-drain current of OECT.

Recently, an integrated wireless mobile health (mHealth) sensing system (**Figures 11C and 11D**) based on laser-engraved graphene for non-invasive cortisol measurement in sweat was developed by Torrente-Rodríguez et al.[104] This wireless sensing device is comprised of a microfluidic module for on-body sweat sampling and a flexible electrode array (including three laser-engraved graphene-based working electrodes, an Ag/AgCl-based reference electrode, and a laser-engraved graphene-based counter electrode) for cortisol recognition. The measurement is based on the competitive binding between sweat cortisol and the cortisol labeled by horseradish peroxidase (HRP) onto the antibody-functionalized graphene electrode. In a 6-day pilot study with a healthy human subject, the developed platform successfully captured the diurnal pattern of sweat cortisol (**Figure 11D**). The sweat cortisol also shows a good correlation with salivary/serum cortisol in a study involving eight healthy subjects (**Figure 11D**). Nonetheless, this platform still requires the addition of external reagents, limiting the real-time in-situ sweat cortisol monitoring. To that end, recently, Wang et al. developed a smartwatch with a flexible aptamer-field-effect transistor (aFET) sensor array for label-free monitoring of cortisol in sweat (**Figure 11E** and **11F**)[105]. A nanometer-

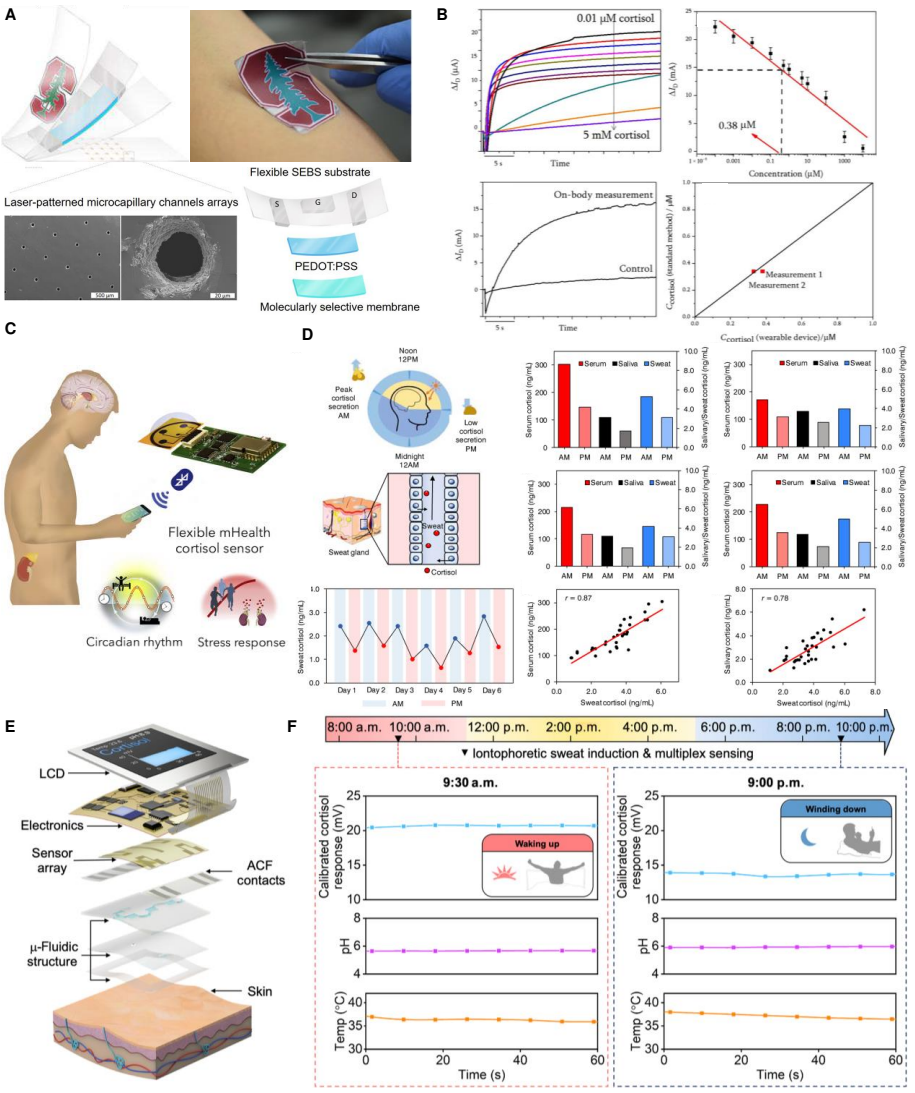

Figure 11. Wearable sensor for cortisol detection. (**A**) The components of the multifunctional layers in flexible OECTs, and (**B**) the analytical performance in sweat cortisol detection. [(A)-(B)] Figure adopted from Ref 103. Reproduced with permission from O. Parlak *et al.,* Sci. Adv. **4** (7), eaar2904 (2018). Copyright 2018 Authors, licensed under a Creative Commons Attribution (CC BY) license. (**C, D**) Laser-engraved graphene-based mHealth device for cortisol measurement in

serum, saliva, and sweat samples from healthy human subjects. [(C)-(D)] Figure adopted from Ref 104. Reproduced with permission from R. M. Torrente-Rodríguez *et al.,* Matter **2** (4), 921-937 (2020). Copyright 2020 Elsevier. (**E, F**) Schematic illustration of the key components of a flexible aptamer-FET-based smartwatch and the representative results for the real-time monitoring of sweat cortisol, pH, and skin temperature during normal daily activities. [(E)-(F)] Figure adopted from Ref 105. Reproduced with permission from B. Wang *et al.,* Sci. Adv. **8** (1), eabk0967 (2022). Copyright 2022 Authors, licensed under a Creative Commons Attribution (CC BY) license.

thin-film of In_2O_3 spin-coated on flexible polyimide was used as the channel layer of FET transduction platform and the aptamer was used as the biorecognition element. The aptamer-FET for cortisol detection is based on the conformational change of the negatively charged aptamer in the presence of cortisol targets. This conformational change induces the surface charge changes in the semiconductor channel, which can be detected by the transfer curve of FET. This fully integrated wearable smartwatch was able to detect cortisol levels in a wide concentration range from 1 pM to 1 μM with a high selectivity and sensitivity. Additionally, it demonstrates the capability for the real-time monitoring of sweat cortisol levels, pH, and skin surface temperature during normal daily activities (**Figure 11F**).

3.3 Electrolyte monitoring

It is well known that one of the early symptoms of COVID-19 is fever. A new study reported that 67/206 patients with low-severity COVID-19 infections experienced diarrhea, and for 19.4% of these cases, diarrhea was the first early symptom.[108] Fever and diarrhea cause the body to lose water and electrolytes rapidly, forcing it to utilize fat and muscle to maintain normal body functions. Due to electrolyte imbalance caused by such losses, fluids and electrolytes must be replenished to prevent dehydration and further complications such as hypokalemia and hyponatremia. Sodium and potassium are two important ions for maintaining electrolyte balance, especially for COVID-19 patients who are undergoing prolonged fever, diarrhea, and normally lost water and electrolytes from skin and stool, which increases the risk of dehydration. Therefore, it is critical to develop a sensor for real-time monitoring of body electrolyte levels, which will help healthcare professionals continuously monitor COVID-19 patients at home and effectively manage the electrolyte balance. Among various biofluids (sweat, saliva, tears, and many others), [109, 110] skin interstitial fluids (ISF) represents a promising biofluid for interface with wearable biosensors for minimally invasive wearable applications.[111-113] Compared to sweat, ISF could provide a rich source of biomarkers, including electrolytes, metabolites, proteins, micronutrients, and hormones for analysis in situ without sample evaporation, contamination, the need for sweating, and the need for storage. Recently, Li et al. developed a microneedle-based potentiometric sensor that can continuously monitor sodium and potassium in skin interstitial fluids.[106] By integrating a miniaturized stainless steel 26 gauge hollow microneedle, this potentiometric sensing system tends to avoid sensor delamination and touching the nerve endings during the sensor implanting, thereby enabling monitoring of the electrolytes in a minimally invasive way like the commercial continuous glucose meter (CGM) (**Figure 12A**). In order to realize the wireless transmission of the measured electrolytes data conveniently and quickly, Zheng et al. reported a wearable microneedle-base gate field effect transistor (FET) sensing system that was minimally invasive for real-time monitoring of sodium in interstitial fluids.[94] This novel biosensor relies on the

microneedle-base extended gate electrode (EG) and reference electrode (RE) that penetrate the skin to access the sodium in the ISF (**Figure 12B**), which shows high stretchability, sensitivity, biocompatibility, and mechanical stability during on-body testing. Integration with wireless communication and the Internet-of-Things cloud, this developed sensor has the potential to enable efficient remote healthcare without face-to-face consultations. Like other biosensors, the interferences from other biomarkers and non-specific adsorption in complex biological environments, like skin ISF, could cause the output noise of the developed ion-selective electrodes. Optimizing the formation of ion-selective membrane and the development of anti-biofouling surface coatings, as detailed in the section summary and perspectives, could resolve these issues. Importantly, due to sensor-to-sensor variations, the sensors usually need to be pre-calibrated before each use to ensure accurate detection using ISE.[114]

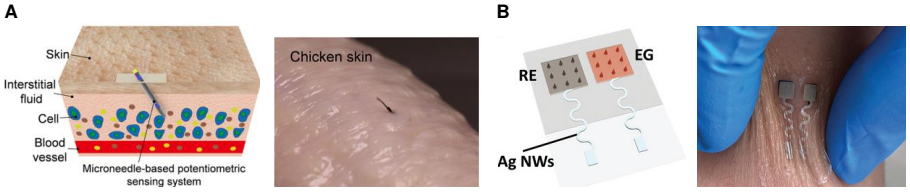

Figure 12. Wearable sensor for electrolytes monitoring. (**A**) Schematic illustration of the microneedle-based potentiometric sensor for electrolytes monitoring in ISF (left). The sensing system implanted in chicken skin (right). Figure adopted from Ref 106. Reproduced with permission from H. Li *et al.,* ACS Sens. **6** (6), 2181-2190 (2021). Copyright 2021 American Chemical Society. (**B**) A microneedle-based FET sensor attached to wrist for continuous monitoring sodium in ISF. Figure adopted from Ref 94. Reproduced with permission from Y. Zheng *et al.,* Adv. Mater. **34** (10), 2108607 (2022). Copyright 2022 Wiley-VCH GmbH.

4. Data analytics and machine learning

4.1 Sensor data analytics

Sensor data analytics is a platform built to analyze the data collected from different sensors. The data is analyzed to gain insight and obtain meaningful understanding by using different metrics. Recent studies have suggested that sensor data analytics is going to play an important role in the wearable sensor area. In particular, Quer et al. developed a smartphone application that collects activity data, as well as self-reported symptoms from individuals to diagnose the COVID-19 infection.[115] They collected the demographic data and sensor data from 54 reported positive and 279 negative participants, including age, resting heart rate (RHR), steps, and sleep activities. To investigate the correlation between sensor data and COVID-19, they proposed a statistical analysis method to estimate the infection status by generating a measure through a weighted combination of the sensor data and comparing it to the baseline value to determine the infection. This study shows that the statistical analysis method reaches an AUC (area under the curve) of 0.80 for COVID-19 detection. The proposed method used 11 hyper-parameters for the calculation, and the weight parameters were optimized by the authors on a given dataset. However, this optimization method is not efficient, and the detection results are sensitive to the settings of the parameters.

Shan et al. developed a nanomaterial-based breath sensor to collect the expiratory gases with different VOCs (volatile organic compounds) and humidity as the input features for the rapid and accurate diagnosis of COVID-19.[116] They followed 49 COVID-19-positive patients, 58 negative individuals, and 33 non-COVID lung infection patients to investigate the sensor responses based on the statistical analysis. The collected data was trained using the discriminant factor analysis (DFA) algorithm, which is a statistical procedure that classifies the unknown individual into a certain group. The experimental results indicate that the proposed method achieves 76% accuracy and an AUC of 0.81 for distinguishing the infection of COVID-19. The nanomaterial-based breath sensor provided a novel solution to identify the COVID-19 infection. However, the statistical method does not have satisfactory performance for sensor data analytics.

4.2 Motion artifacts

Motion artifacts create a unique challenge for utilizing the data from a sensor for further analysis, such as for estimation or classification tasks. They are especially critical when measuring physiological parameters, such as the respiration rate, heart rate, blood oxygen level, and body temperature. Motion artifacts can appear in many forms, the most common ones are noise and interference. These artifacts often come from the body movements, changes in body position or posture, or contact pressure between the sensor and skin. They often affect substantially the overall performance of a wearable device. To effectively address the issue, it is important to understand the source of motion artifacts and the data analytic techniques that can mitigate the effects of motion artifacts. The processing to handle motion artifacts can be problem dependent and should be properly designed in order to fully utilize the data collected by a sensor.

A common approach to limit the detrimental effects from artifacts is by filtering. The goal is to separate the desired signal from the noise generated by motion artifacts. A filter can be designed with a passband over the frequency region where the useful information lies and eliminate all other frequency content that may be due to noise or interference from the unrelated activities.[117] Various filtering methods have been proposed in the literature, including low-pass filters, high-pass filters, band-pass filters, and adaptive filters. Tanweer et al. presented a filtered-X least mean square (FX-LMS) adaptive noise cancellation algorithm to reduce the motion artifacts from the sensor data during intensive exercise[118], which enhanced the signal quality for accurate heart rate estimation. In another study, Zhang et al. proposed a general framework called TROIKA[119]. It uses a combination of filtering, spectral analysis, and time-frequency analysis techniques to reduce motion artifacts. This framework is shown to be able to improve the accuracy and reliability of heart rate monitoring using the wearable photoplethymogram (PPG) sensors.

Data fusion and sensor fusion are also primary techniques to enhance the overall performance of a wearable device by combining useful data from multiple sensors. They can help to detect and compensate for the motion artifacts by exploiting additional contextual information. Yousefi et al. presented a motion-tolerant adaptive algorithm for wearable PPG biosensors based on particle filtering[120]. It combines data from the PPG sensors and the three-axis accelerometer to estimate the heart rate. The proposed method improved the heart rate estimation accuracy and demonstrated the potential of data fusion techniques for wearable sensor applications. Bian et al. presented a fusion method for heart rate, respiration rate, and motion measurements from a wearable sensor system[121]. The method combines data from multiple wearable sensors, including the PPG,

respiration, and accelerometer sensors, and performs a regression method to estimate the energy expenditure. These methods illustrated that data fusion and sensor fusion can play a critical role in handling motion artifacts.

Machine learning technique has been an active area of research in recent years and shown promising performance in addressing motion artifact problems. It enables the extraction of relevant features and patterns from the sensor data, leading to more accurate identification and correction of motion artifacts. The paper[121] explored the use of machine learning method to estimate the respiration rate from noisy signals. It investigated several machine learning algorithms, including the decision trees, k-nearest neighbors (KNN), and support vector machine (SVM), to identify and correct the motion artifacts from the observations. Cho et al. introduced a robust method by tracking the respiration rate in the scenes having high-dynamic range, through mobile thermal imaging and machine learning techniques[122]. It employed a combination of feature extraction and an SVM classifier to identify the pattern of respiration to mitigate the motion artifacts, resulting in improved reliability of the respiration rate estimation.

Despite the potential of different approaches and techniques in addressing the motion artifacts, there remain challenges in the development to effectively handle the motion artifacts. For instance, developing the algorithms that can adapt to various individual characteristics may be very challenging, since the processing method of the signals from different ages, genders, and body builds might be different. In addition, the methods for mitigating motion artifacts need to be computationally efficient and can be implemented on a wearable device that has limited resources. Future research should focus on refining data analytics techniques from motion artifact correction and exploring new directions to solve the motion artifact challenges in wearable devices.

4.3 Data preprocessing methods

Sensors are becoming increasingly essential, especially in monitoring the key physiological parameter of diseases, such as vital signs and symptoms. Early detection of the COVID-19 infection relies on the extraction of useful information from the raw data collected from sensors. Sensor data are often noisy, susceptible to interference, and could have redundant information. Indeed, the background and environmental noises are the key challenges to mitigate in order to have the sensor data to be useful. The irrelevant components in the sensor data will increase the computational complexity and reduce the detection performance. A suitable data preprocessing method can significantly improve the precision of detecting COVID-19 infection. Therefore, some researchers are focusing on the preprocessing methods for the sensor data, not only for extracting the relevant and independent information, but also for providing better inputs/features to a machine learning algorithm that can produce more accurate results. Wu et al. started with 74 COVID-19 related features in a set of raw data, including the symptoms, blood test, biochemical examination, etc.[123] The features are not independent. They studied the similarity in the distribution of the features and removed the features that were significantly correlated to reduce the redundant information. Eventually, the number of features was reduced to only 37. Then the reduced feature set is utilized in different machine learning algorithms for COVID-19 detection. It has improved computational efficiency and performance accuracy. Dairi et al. addressed the problem of reducing the dimensionality of the input features by using a variational autoencoder (VAE) rather than the traditional principal component analysis (PCA).[124] Although PCA is faster and computationally

efficient, VAE is capable of modeling complex non-linear problems and ensuring the low dimensional latent space represents the most important features. They trained the VAE network for feature dimensionality reduction and relevant non-linear information extraction hidden in the blood test data. The VAE network appears to be quite effective.

VAEs and PCA are both dimensionality reduction methods. PCA is a traditional statistical method that uses orthogonal transformation to convert a large set of variables into a smaller one, called principal components. PCA is linear and only captures the global structure of the data. VAE is a type of generative model that uses machine learning techniques to learn complex, non-linear transformations for the data dimensional reduction. The VAE networks appear more effective than PCA. Because PCA is limited to linear transformations, only capturing linear relationships between variables, and it only works well when the data follows Gaussian distribution. In contrast, VAE method can identify the non-linear associations throughout the entire dataset. The non-linear capability enables VAE to more accurately construct highly complex data distributions, which makes it more suitable for a wide range of data types.

The VAE networks also have the unique property of learning a structured and consistent latent space, a feature arising from the machine learning approach that is trained to understand a distribution over the latent space. This attribute is especially beneficial for feature extraction, as it enables the model to create a useful latent space that can be utilized for classification. On the other hand, the latent space of PCA is not constructed and consistent between variables, resulting in inadequate feature extraction performance for complex data distribution.

In conclusion, the VAE presents several advantages over the traditional linear methods like PCA, especially when dealing with complex, high-dimensional data. The non-linear modelling capability of VAEs allows them to construct important and accurate relationships from the data. Consequently, the VAE network is quantitatively more effective than PCA.

It is common in a medical dataset that encounters numerous missing data points and has imbalanced data observations, which may cause a machine learning model in producing false detection. Mohammedqasem et al. proposed an oversampling algorithm that addresses the data imbalance issue by increasing minority samples through synthetic samples.[125] They randomly interpolated the homogeneous neighboring samples to generate new synthetic samples. In addition, they analyzed the sample distribution to remove the overlapping samples and noise samples before including the synthetic data in the minority class. Different from using the self-reported symptoms, researchers also reported the ability to early detect COVID-19 infection by collecting the vital signals, such as heart rate and respiratory rate. Challenges remain in addressing the noisy background while recording vital signals. Ni et al. exploited the time-frequency features to separate coughing from other common daily activities.[45] They preprocessed the raw data by transforming it into a time series and spectrogram representation by using the Fast Fourier Transform (FFT) with the Hanning window. Then the spectrogram is used to train the machine learning model, which ensures the robustness of the input features and improves the performance in classification.

4.4 Machine learning-enabled early detection and medical interventions

To understand the mechanism of a new virus, such as COVID-19, machine learning models may capture valuable information related to the symptoms. If we utilize the interpretation from the machine learning model at the early stage, there will be a chance to mitigate the severity of the pandemic. Plenty of analysis methods and predictive models have emerged to extract key features from sensor data or image data. For example, a decision tree model that distinguishes the abnormal coughing data and combines other symptoms can determine whether the patient is infected by COVID-19 or not. In addition, a deep learning model is able to detect unusual parts from computerized tomography (CT) scan images. Machine learning models that achieve high accuracy provide early identification and monitoring of potential pandemic cases. Therefore, it is expected that the development of effective machine-learning methods will help early detection and medical interventions, especially since a number of machine-learning algorithms have been proposed to analyze medical cases during the past few years. In this section, we will mainly review the recent development of machine learning algorithms for monitoring some virus cases, predicting the severity of a patient's illness, and early identifying COVID-19 patients. **Table 3** summarizes the results of COVID-19 detection and classification that are reported in the literature by different machine learning algorithms.

Table 3. Classification performance regarding the early detection and severity of COVID-19 infection. 'CNN' and 'SVM' denoted 'Convolutional Neural Network' and 'Support Vector Machine', respectively. '*' represents the AUC value. 'NA' means the results did not get reported.

Algorithm	Dataset	Precision	Recall/AUC	Ref.
Statistical Analysis	333 Patients Collection	NA	0.80*	[115]
Decision Tree	Albert Einstein Hospital	0.88	0.75	[123]
	Open Research Dataset	0.92	0.95*	[126]
Random Forest	Electronic Health Records	0.95	0.97	[127]
	53 Patients Collection	0.7	NA	[128]
SVM	Albert Einstein Hospital	0.98	0.99	[124]
	JinYinTan Hospital	0.94	0.95	[129]
MLP	231 Patients Collection	NA	0.74	[130]
CNN	20 Patients Collection	0.87	0.98	[45]
	Albert Einstein Hospital	0.96	0.98	[131]

4.4.1 Decision Tree

A decision tree model is a tree-like structure in which the node represents the outcome of a test, and the leaf represents a class label (**Figure 13A**). The decision tree is widely used in classification and regression problems. It is well known that the decision tree can be easily visualized and interpreted by exploiting the tree-based decision rules from the data features. Recently, Wu et al. applied the decision tree algorithm to the COVID-19 severity prediction task for further analysis of the most relevant features.[94, 123] The interpretation shows that the decision tree recognized that the NTproBNP, CRP, and ALB (Albumin) are the most important features. In addition, the results indicate that the decision tree has less tolerance for a high level of NTproBNP. However, the decision tree model makes the wrong diagnosis, which is unable to identify two severe patients among nine patients in the testing set. Otoom et al. explained that the decision tree algorithm makes

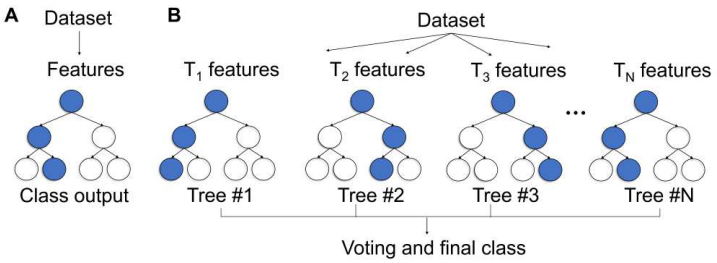

Figure 13. (A) Basic framework of the decision tree algorithm. **(B)** Structure of the random forest algorithm, where "T_N" denotes the features for the "N"th tree.

the prediction using only one feature in each decision node by computing all training examples and selecting one maximum information gain value.[126] Yang et al. proposed a clinically operable decision tree to rapidly identify whether the patient is at high risk of death so that the patient can get a high-priority treatment and urgent care.[132] They first built a two-stage decision tree, including three biomarkers, neutrophil-to-lymphocyte ratio, CRP, and lactic dehydrogenase. Then the cross-validation method was applied to trim the full tree, and they chose the smallest complexity parameter to build a simple and meaningful decision tree. The model achieves 0.98 accuracies in the 2,169 COVID-19 patients' dataset. The decision tree algorithm is easy to interpret and understand, but not appropriate for large-scale datasets and applications.

4.4.2 Random Forest

Random Forest (RF) is an ensemble learning method for classification and regression problems. It utilized a bagging strategy and feature randomness to create an individual tree from which to form multiple decision trees using the same learning algorithm (**Figure 13B**). Random forest algorithms can achieve high accuracy results in many classification cases without having many hyper-parameters. It is widely used in many simple classification problems and is an alternative to the decision tree algorithm. However, the random forests algorithm is much more difficult to interpret because the model sometimes contains hundreds of decision trees. Wu et al. recently employed the random forests algorithm in COVID-19 severity prediction for recognizing the permutation of the important features.[123] The CRP2 and NTproBNP are identified as the most important features for the prediction by the random forests algorithm. Compared to the decision tree algorithm, they claimed that the F1 score is slightly higher on the classification task. However, both the random forest and decision tree algorithms misclassified two severe COVID-19 patients. Gao et al. presented a mortality risk prediction model for COVID-19 (MRPMC) by combining decision tree, random forest, and other machine learning algorithms to build a classification model, which is able to predict physiological deterioration and death up to 20 days in advance.[127] They proclaimed that the model achieves an AUC of 0.97 in an internal validation cohort and potentially improves the monitoring and recovery for high-risk COVID-19 patients. The random forest machine learning algorithm also shows great ability to the regression problem. Yesilkanat et al. investigated the performance of estimating the number of COVID-19 cases for the near future by utilizing the random forest algorithm.[133] They used 1,500 decision trees and 3 splits at the node points of the tree to build the random forest model. The comparative results show that the random forest machine learning algorithm has produced very accurate results in estimating the number of

COVID-19 cases during 1-17 June 2020, which achieves an average of 0.914 R^2 values and enables to prevent the sudden epidemic. However, the method would be more convincing if the data period could be longer in the evaluation process. Recently, Barbosa et al. proposed a web solution to rapidly diagnose COVID-19 by applying a random forest algorithm to the blood test data.[134] The diagnosis chose 41 blood test features among the total 107 features, such as CRP, Creatinine and D-Dimer, etc. It is quite effective and recommended by the Ministry of Health as an initial clinical approach for diagnosing COVID-19. They build the random forest model using 90 and 100 trees, which is able to achieve an accuracy above 90% and a kappa statistic above 0.80. They claimed that the task of diagnosing COVID-19 is harder than indicating the type of hospitalization using the same blood test features. The proposed system is a web solution that is flexible and available to access online for the diagnosis. Shen et al. suggested that the proteomic and metabolomic profiling of sera are the keys to early detection and effective treatment of severe COVID-19 patients.[128] They collected 46 positive patients and 53 negative individuals to measure the proteomic and metabolomic as the input features for training a machine learning model. The random forest algorithm is employed to evaluate the patients, and further evaluate the severity of the patients into the mild, non-severe, and severe categories. The model was validated using 10 independent patients, and 7 of them were correctly detected with COVID-19. The limitation of this study is the insufficient amount of clinical data. However, the model revealed the characteristic protein and metabolite changes are the critical biomarkers for the evaluation of the severity in the infection.

4.4.3 Support Vector Machines (SVMs)

SVM is a machine learning model with associated learning algorithms that are used for classification and regression analysis. The objective of the SVM algorithm is to find a hyperplane in an N-dimensional space that maximizes the distance between the data points of different classes (**Figure 14A**). SVM maps the data to high-dimensional feature space and determines the decision boundaries to classify the data points. SVM is effective for operation in high dimensional space, has high accuracy for classification problems, and is memory efficient. It is not only widely used in signal classification problems but also performs well in image classification problems. Therefore, recent studies present much progress in biomedical-related topics using the SVM algorithm. Dairi et al. addressed the problem of detecting COVID-19 infection using the blood test features and unsupervised SVM algorithm.[124] They first extracted the features from the data using a variational autoencoder (VAE), aiming to reduce the dimensionality of the data features and encode a new data representation from the blood test samples. Then the SVM is applied to the output of the VAE without using any label, which determines a hyperplane that is as close as possible to the normal samples. They claimed that the SVM algorithm achieves 99.3% AUC of detection accuracy in evaluating 1,700 samples of blood tests. The innovation of this paper is that they proposed a method to detect COVID-19 in an unsupervised manner using the SVM algorithm and blood test samples. The SVM algorithm is also frequently designed to recognize and discriminate the severity of the diseases. Shi et al. proposed an enhanced SVM algorithm to determine the severity of COVID-19 by utilizing clinical data, such as patient basic information and hematological indices.[135] The proposed method first normalized the data features and mapped them from the input space to the high-dimensional feature space. The Slime Mould Algorithm (EMA) is applied to convert the optimal feature into the binary space using the sigmoid function,

and the feature is considered meaningful to use if it is less than the threshold. The SVM is then trained to obtain a high-quality classification of the COVID-19 severity using binary features. The extensive experimental results show that the proposed framework achieves 91.09% accuracy in discriminating the severity of 51 COVID-19 patients. The ablation studies performed a further analysis of the components in the framework, which proved that the SVM algorithm is more accurate compared to the KNN (K Nearest Neighbor) algorithm. To rapidly recognize the potential COVID-19 cases from the real-time data of symptoms, Otoom et al. built a framework to collect data and compare the performance of the SVM algorithm with other different machine learning algorithms.[126] The proposed system collected real-time symptoms using wearable sensors, including fever, cough, shortness of breath, and 80 relevant symptoms. The collected symptom data are ranked and reduced to the 20 most indicative symptoms and uploaded to an internet-based system for early identification of suspected COVID-19 cases through the SVM machine learning algorithm. The SVM algorithm achieves 92.95% accuracy and 93.9% ROC (Receiver Operating Characteristic) area, while the decision tree algorithm reaches 70.73% accuracy and 70.1% ROC area. The results suggested that the proposed method provides effective and accurate identification of potential cases of COVID-19, and the framework is suitable for the patient to track and evaluate their health status at the earliest convenience. The symptom features are the critical elements to the training of the machine learning model, and further the optimization of the performance of the model. Xiong et al. designed a feature selection system to extract the 23 most critical features from

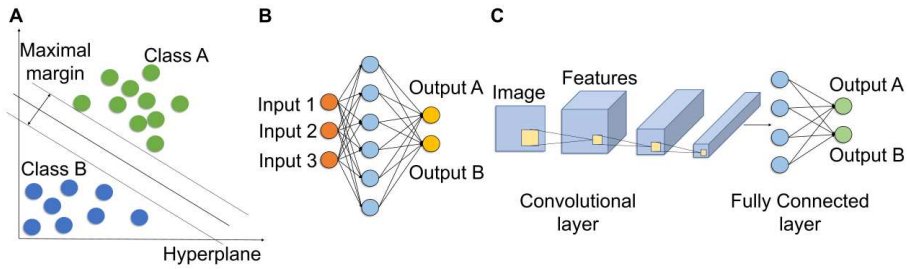

Figure 14. (**A**) Illustration of the SVM algorithm. (**B**) Basic structure of the MLP network. (**C**) Architecture of the CNN.

the initial 86 symptom features by using the LassoCV method, Spearman's rank correlation, and expert opinions.[129] The selected 23 features were processed by the SVM algorithm in predicting COVID-19 severity, and 287 patients were categorized as non-severe and severe cases. With a more accurate selection process, the SVM model achieves 94.80% AUC and 93.90% accuracy. In addition, the proposed method suggested that the chest-CT had the highest importance in the diagnosis of COVID-19 severity, and the following features were neutrophil to lymphocyte ratio. Based on the above studies, the SVM algorithm could be a powerful predictive tool to identify the severity of the patient for early detection of the disease.

4.4.4 Neural Networks (NNs)

Neural networks are the most popular and most well-known machine learning algorithm that is used extensively for the classification and regression problems. There are two main types of neural

networks in general, Multiple Layer Perceptrons (MLPs) and Convolutional Neural Networks (CNNs), which provide flexibility in a wide range of biomedical problems. The MLP algorithm consists of one or more layers of neurons and is suitable for classification problems where the inputs are tabular datasets (**Figure 14B**), such as blood test features and symptom features. The CNNs were developed for the image classification problems that mapped the image data to an output variable (**Figure 14C**). In general, the CNNs perform well with data that contains spatial information, whereas MLPs are appropriate with temporal and documental data. Valle et al. implemented an MLP model to investigate whether the inflammatory cytokine levels can help to predict the association between the diseases and COVID-19 severity.[130] They followed 1,484 patients who were suspected or confirmed of having COVID-19 with clinical information and laboratory test results. Then the MLP model is applied to test the association of the cytokine values with the patient demographics. Compared to other different variables, the output of the model shows that the cytokine level is significantly higher for the patients who test positive for COVID-19 infection. In addition, the neural network model suggested that chronic kidney disease (CKD) and age were strongly correlated with the risk of death from COVID-19. Due to the limitation of clinical decisions, Alakus et al. proposed a prediction system for detecting the infection of COVID-19 using various deep-learning models.[136] In this study, they trained the machine learning model with 18 laboratory findings from 600 patients, such as red blood cells, hemoglobin, monocytes, leukocytes, etc. The architecture of the MLP model is comprised of 3 layers and a total of 56 neurons, while the CNN model is built by 2 convolutional layers and 2 fully connected layers. To evaluate the performance of each machine learning model, they compared the accuracy, F1-score, and AUC values using the 10-fold cross-validation approach. In terms of the evaluated performance, they claimed that the accuracy of the CNN model is slightly higher than the MLP model, which is 88% and 86% in accuracy, respectively. Further studies proved that neural networks are able to precisely predict the infection of COVID-19. However, a limitation of the study is that the data size is relatively small, and some laboratory findings are missing for some patients. On the contrary, Ni et al. integrated the mechanoacourstic (MA) sensors and convolutional neural networks to the monitoring of COVID-19 infections in sick and healthy patients.[45] They incorporated an MA sensor, Bluetooth device, cloud-based data transmission, and automatic data preprocessing framework to build a health monitoring system. Unlike the previous studies, this paper focuses on capturing the subtle vibrations of the skin and collecting the sensor signals as input features, including the signals of tapping, coughing, laughing, throat clearing, and speaking. Rather than directly using the raw signal data from the MA sensor, the signal preprocessing step of converting the raw data to spectrogram is found to be the most important part to improve the accuracy. Distinguishing the actual coughs from other cough-like signals, the CNN is applied for further analysis. They collected the daily behavior signals from 10 healthy volunteers and 10 COVID-19 patients for training the CNN model. The model starts with 3 convolutional layers, followed by a ResNet-50 network, and it achieves an accuracy of 0.90 for coughing signals using the spectrogram features. With the long-term monitoring, they suggested that coughing and respiration rates are the potentially important biomarkers that can identify the COVID-19 patients and healthy subjects.

5. Summary and Perspectives

In addition to re-exposing many vulnerabilities of traditional health care practices, the unexpected outbreak of COVID-19 also greatly amplified the importance and the appeal of remote health care

and propelled the research toward this new paradigm of medicine. A particularly appealing body of recent research efforts involves wearable sensors capable of capturing a vast range of biomarkers of human physiology. In this review, we have reviewed the recent progress in wearable sensor research in consideration of the COVID-19 pandemic and its implications. The first part of this review was dedicated to wearable biophysical sensors for monitoring a variety of conventional biomarkers and vital signs, including body temperature, respiration rate, blood oxygen saturation, heart rate, and heart rate variability. These biophysical signals have been extensively studied, with a significant body of research supporting that they can be reliable predictors of outcomes and symptoms of diseases, including COVID-19. The second part of this report was devoted to the recent advances in wearable biochemical sensors, an emerging field that promises to make biochemical sensing continuous, pain-free, and easy-to-use. Unlike biophysical sensors, biochemical sensors can provide a direct assessment of biochemistry and metabolism at the molecular level. Monitoring of biochemistry content such as electrolytes, cytokines, and cortisol can provide crucial insights towards effective therapeutics for COVID-19. The third and final portion of the review focused on the recent developments in data analytics and machine learning methods used to perform predictive assessments on data collected from biophysical and biochemical sensors. These methods offer tremendous value for remote medicine as they can support healthcare professionals in medical decision-making, early detection, and prevention of disease.

Recently, there have been many demonstrations of novel sensing devices and examples of integration of some of the biophysical and biochemical sensing concepts discussed in this work into wearables and accessories used daily by humans. These unique devices include (in addition to the skin patches and bandages already discussed in this review) face masks for monitoring breathing patterns, pathogens, inflammation markers, contact lenses for measuring cortisol, glucose, intraocular pressure, and dental chips for tracking therapeutic drugs.[68] Some of these devices have already been FDA-approved and introduced to the general consumer market,[137] which further implies the imminent popularization of advanced state-of-the-art wearable sensors for the general public.

For future development of advanced wearable sensors, integrating biophysical and biochemical sensors in a hybrid platform is very appealing, because this will greatly enhance the performance and reduce inaccuracies by introducing data redundancy and improving data diversity. More specifically, integrated hybrid sensors will be crucial for data analytics and machine learning methods, as they have been shown to generally benefit from increased number of features and data diversification (Gong et al.).[138] In the past few years, such platforms have emerged including a hybrid biochemical (lactate) and ECG monitoring system.[139] and a sensor patch for 3D imaging of total hemoglobin and core temperature.[83] We believe that combining biochemical cytokine, cortisol, and electrolyte sensors with PPG pulse oximetry would be a highly promising hybrid scheme, due to the low cost and complexity of the associated biophysical sensing hardware and the ability to continuously and accurately monitor many relevant biomarkers that have been shown to be related to infectious diseases such as COVID-19.

Despite these recent advances in wearable sensors, the continuous biophysical and biochemical monitoring in COVID-19 patients still faces the following challenges, which require future developments. First, non-specific adsorptions and biofouling. The non-specific adsorptions could

block the sensor surface to cause biofouling and influence its long-term continuous monitoring. To address this issue, the recently developed antibiofouling coatings of zwitterionic polymers and polyacrylamide hydrogels could be used to reduce biofouling.[140, 141] For these applications, the surface densities of the sensor receptors and antifouling coatings should be systematically optimized to ensure that the resultant sensors perform optimally (i.e., with high sensitivity, selectivity, and fast response time) in targeted biofluids. In addition to the antibiofouling coatings, wearable microfluidics represents another option for minimizing biofouling for wearable devices. For example, the recently developed wearable microfluidics isolate and transport the biofluid,[142, 143] like sweat, immediately from the skin once it emerges from the sweat gland, thereby protecting the sensors from biofouling associated with debris and oils on the skin surface or from environmental contaminants.

Second, continuous monitoring in skin ISF. Compared with other biofluids, like sweat, tears, and saliva, the skin ISF, which is formed through plasma extravasation from continuous capillaries and surrounds tissues and cells, presents an emerging biofluid for health monitoring and clinical medicine due to the similarities and/or correlation of biomarkers in skin ISF and that in plasma.[144] This biofluid is a rich source of biomarkers, including proteins, nutrients, metabolites, and hormones.[144] Importantly, many low molecular weight analytes such as metabolites (glucose and lactate) and nutrients have essentially equivalent concentrations in plasma and ISF due to the high density and surface-to-volume ratio of continuous capillaries, blood pressure forces, and diverse biomarker transport routes from plasma to ISF. The ISF/plasma concentration ratio for higher molecular weight analytes, such as proteins and lipids, ranges from 0.9 to 0.14,[144] depending on the analyte's molecular weight. Despite that, the current wearable sensors for continuous monitoring of biomarkers in skin ISF are only limited to a handful of biomarkers, including electrolytes and metabolites. The continuous monitoring beyond these biomarkers represents a future direction, in particular, the monitoring of hormones, proteins, and nutrients for chronic disease monitoring and management, like chronic kidney disease and cardiovascular disease.

Finally, the limited amount of data from human subjects for the training of ML algorithm. Collecting data from as many diverse subjects as possible is essential to build machine learning models for accurate results. Otherwise, learning from a limited number of subjects may fail to generalize, leading to uncertain performance. The training data is the most critical element in developing machine learning models. The challenge for machine learning is insufficient training data and inconsistent responses from individuals. One possibility of having extensive learning data is through open-source sharing, where various research groups post their wearable data for free access. However, this approach may be subject to data privacy issues, and the details related to the data collected and subjects may not be available.[145] As a result, it may not be suitable for specific applications. Another approach for handling the small dataset problem is by augmenting the data. Augmentation can be performed in the time domain through isolating signals, adding Gaussian noise, data shifting, or their combinations. These techniques for augmentation have been widely used in the machine-learning community to create additional data for model training. It has been demonstrated that data augmentation can help to increase the model capability. Indeed, augmented data can be made by using generative adversarial networks (GANs),[146] which is an approach to generating new synthetic data for training ML models. It helps to produce more data and train accurate models without exposing the actual user data.

Acknowledgments

We acknowledge the funding support by the University of Connecticut start-up fund and NSF ECCS-2113736.

Conflict of Interest

The authors declare no conflict of interest.

References

1. W. J. Wiersinga, A. Rhodes, A. C. Cheng, S. J. Peacock and H. C. Prescott, "Pathophysiology, transmission, diagnosis, and treatment of coronavirus disease 2019 (COVID-19): a review" JAMA **324** (8), 782-793 (2020).
2. T. R. Ray, J. Choi, A. J. Bandodkar, S. Krishnan, P. Gutruf, L. Tian, R. Ghaffari and J. A. Rogers, "Bio-integrated wearable systems: a comprehensive review" Chem. Rev. **119** (8), 5461-5533 (2019).
3. J. Heikenfeld, A. Jajack, J. Rogers, P. Gutruf, L. Tian, T. Pan, R. Li, M. Khine, J. Kim and J. Wang, "Wearable sensors: modalities, challenges, and prospects" Lab Chip **18** (2), 217-248 (2018).
4. W. Gao, H. Ota, D. Kiriya, K. Takei and A. Javey, "Flexible electronics toward wearable sensing" Acc. Chem. Res. **52** (3), 523-533 (2019).
5. Z. Lou, L. Wang and G. Shen, "Recent advances in smart wearable sensing systems" Adv. Mater. Technol. **3** (12), 1800444 (2018).
6. Y. Ling, T. An, L. W. Yap, B. Zhu, S. Gong and W. Cheng, "Disruptive, soft, wearable sensors" Adv. Mater. **32** (18), 1904664 (2020).
7. J. R. Sempionatto, J. A. Lasalde-Ramírez, K. Mahato, J. Wang and W. Gao, "Wearable chemical sensors for biomarker discovery in the omics era" Nat. Rev. Chem. 1-17 (2022).
8. H. C. Ates, P. Q. Nguyen, L. Gonzalez-Macia, E. Morales-Narváez, F. Güder, J. J. Collins and C. Dincer, "End-to-end design of wearable sensors" Nat. Rev. Mater. 1-21 (2022).
9. C. Wang, E. Shirzaei Sani and W. Gao, "Wearable bioelectronics for chronic wound management" Adv. Funct. Mater. **32** (17), 2111022 (2022).
10. J. Kim, A. S. Campbell, B. E.-F. de Ávila and J. Wang, "Wearable biosensors for healthcare monitoring" Nat. Biotechnol. **37** (4), 389-406 (2019).
11. J. J. Kim, Y. Wang, H. Wang, S. Lee, T. Yokota and T. Someya, "Skin electronics: next-generation device platform for virtual and augmented reality" Adv. Funct. Mater. **31** (39), 2009602 (2021).
12. P. Zhu, H. Peng and A. Y. Rwei, "Flexible, wearable biosensors for digital health" Med. Nov. Technol. Devices. 100118 (2022).
13. Y. Khan, A. E. Ostfeld, C. M. Lochner, A. Pierre and A. C. Arias, "Monitoring of vital signs with flexible and wearable medical devices" Adv. Mater. **28** (22), 4373-4395 (2016).
14. Y. J. Hong, H. Jeong, K. W. Cho, N. Lu and D. H. Kim, "Wearable and implantable devices for cardiovascular healthcare: from monitoring to therapy based on flexible and stretchable electronics" Adv. Funct. Mater. **29** (19), 1808247 (2019).
15. A. Ahmad Tarar, U. Mohammad and S. K Srivastava, "Wearable skin sensors and their challenges: A review of transdermal, optical, and mechanical sensors" Biosensors **10** (6), 56 (2020).

16. S. Chen, J. Qi, S. Fan, Z. Qiao, J. C. Yeo and C. T. Lim, "Flexible wearable sensors for cardiovascular health monitoring" Adv. Healthc. Mater. **10** (17), 2100116 (2021).
17. Y. Liu, D. Shukla, H. Newman and Y. Zhu, "Soft wearable sensors for monitoring symptoms of COVID-19: A review" Prog. biomed. eng. (2021).
18. S. Mirjalali, S. Peng, Z. Fang, C. H. Wang and S. Wu, "Wearable Sensors for Remote Health Monitoring: Potential Applications for Early Diagnosis of Covid-19" Adv. Mater. Technol. **7** (1), 2100545 (2022).
19. S. Afroj, L. Britnell, T. Hasan, D. V. Andreeva, K. S. Novoselov and N. Karim, "Graphene-Based Technologies for Tackling COVID-19 and Future Pandemics" Adv. Funct. Mater. **31** (52), 2107407 (2021).
20. L. Y. Mortenson, P. N. Malani and R. D. Ernst, "Caring for someone with COVID-19" JAMA **324** (10), 1016-1016 (2020).
21. S. Tharakan, K. Nomoto, S. Miyashita and K. Ishikawa, "Body temperature correlates with mortality in COVID-19 patients" Crit Care **24** (1), 1-3 (2020).
22. C. Childs, "Maintaining body temperature" Alexander's Nursing (2011).
23. E. Bridges and K. Thomas, "Noninvasive measurement of body temperature in critically ill patients" Crit. Care Nurse **29** (3), 94-97 (2009).
24. M. Sang, K. Kang, Y. Zhang, H. Zhang, K. Kim, M. Cho, J. Shin, J. H. Hong, T. Kim, S. K. Lee, W.-H. Yeo, J. W. Lee, T. Lee, B. Xu and K. J. Yu, "Ultrahigh Sensitive Au-Doped Silicon Nanomembrane Based Wearable Sensor Arrays for Continuous Skin Temperature Monitoring with High Precision" Adv. Mater. **34** (4), 2105865 (2022).
25. M. Li, J. Chen, W. Zhong, M. Luo, W. Wang, X. Qing, Y. Lu, Q. Liu, K. Liu, Y. Wang and D. Wang, "Large-area, wearable, self-powered pressure–temperature sensor based on 3D thermoelectric spacer fabric" ACS Sens. **5** (8), 2545-2554 (2020).
26. D. S. Moran and L. Mendal, "Core temperature measurement" Sports Med . **32** (14), 879-885 (2002).
27. H. Jeong, J. Y. Lee, K. Lee, Y. J. Kang, J.-T. Kim, R. Avila, A. Tzavelis, J. Kim, H. Ryu, S. S. Kwak, J. U. Kim, A. Banks, H. Jang, J.-K. Chang, S. Li, C. K. Mummidisetty, Y. Park, S. Nappi, K. S. Chun, Y. J. Lee, K. Kwon, X. Ni, H. U. Chung, H. Luan, J.-H. Kim, C. Wu, S. Xu, A. Banks, A. Jayaraman, Y. Huang and J. A. Rogers, "Differential cardiopulmonary monitoring system for artifact-canceled physiological tracking of athletes, workers, and COVID-19 patients" Sci. Adv. **7** (20), eabg3092 (2021).
28. F. Ershad, A. Thukral, J. Yue, P. Comeaux, Y. Lu, H. Shim, K. Sim, N.-I. Kim, Z. Rao, R. Guevara, L. Contreras, F. Pan, Y. Zhang, Y.-S. Guan, P. Yang, X. Wang, P. Wang, X. Wu and C. Yu, "Ultra-conformal drawn-on-skin electronics for multifunctional motion artifact-free sensing and point-of-care treatment" Nat. Commun. **11** (1), 1-13 (2020).
29. K. Lee, X. Ni, J. Y. Lee, H. Arafa, D. J. Pe, S. Xu, R. Avila, M. Irie, J. H. Lee, R. L. Easterlin, D. H. Kim, H. U. Chung, O. O. Olabisi, S. Getaneh, E. Chung, M. Hill, J. Bell, H. Jang, C. Liu, J. B. Park, J. Kim, S. B. Kim, S. Mehta, M. Pharr, A. Tzavelis, J. T. Reeder, I. Huang, Y. Deng, Z. Xie, C. R. Davies, Y. Huang and J. A. Rogers, "Mechano-acoustic sensing of physiological processes and body motions via a soft wireless device placed at the suprasternal notch" Nat. Biomed. Eng. **4** (2), 148-158 (2020).
30. D. Seok, S. Lee, M. Kim, J. Cho and C. Kim, "Motion artifact removal techniques for wearable EEG and PPG sensor systems" Front. Inf. Technol. **2**, 685513 (2021).

31. D. J. Miller, J. V. Capodilupo, M. Lastella, C. Sargent, G. D. Roach, V. H. Lee and E. R. Capodilupo, "Analyzing changes in respiratory rate to predict the risk of COVID-19 infection" PloS one **15** (12), e0243693 (2020).
32. A. Natarajan, H.-W. Su and C. Heneghan, "Assessment of physiological signs associated with COVID-19 measured using wearable devices" NPJ Digit. Med. **3** (1), 1-8 (2020).
33. A. Natarajan, H.-W. Su, C. Heneghan, L. Blunt, C. O'Connor and L. Niehaus, "Measurement of respiratory rate using wearable devices and applications to COVID-19 detection" npj Digit. Med. **4** (1), 1-10 (2021).
34. N. A. Chatterjee, P. N. Jensen, A. W. Harris, D. D. Nguyen, H. D. Huang, R. K. Cheng, J. J. Savla, T. R. Larsen, J. M. D. Gomez, J. M. Du-Fay-de-Lavallaz, R. N. Lemaitre, B. McKnight, S. A. Gharib and N. Sotoodehnia, "Admission respiratory status predicts mortality in COVID-19" Influenza Other Respir. Viruses **15** (5), 569-572 (2021).
35. Y. Liu, L. Zhao, R. Avila, C. Yiu, T. Wong, Y. Chan, K. Yao, D. Li, Y. Zhang, W. Li, Z. Xie and X. Yu, "Epidermal electronics for respiration monitoring via thermo-sensitive measuring" Mater. Today Phys. **13**, 100199 (2020).
36. Z. Liu, Z. Li, H. Zhai, L. Jin, K. Chen, Y. Yi, Y. Gao, L. Xu, Y. Zheng, S. Yao, Z. Liu, G. Li, Q. Song, P. Yue, S. Xie, Y. Li and Z. Zheng, "A highly sensitive stretchable strain sensor based on multi-functionalized fabric for respiration monitoring and identification" Chem. Eng. J. **426**, 130869 (2021).
37. M. Zhang, C. Wang, H. Wang, M. Jian, X. Hao and Y. Zhang, "Carbonized cotton fabric for high-performance wearable strain sensors" Adv. Funct. Mater. **27** (2), 1604795 (2017).
38. M. Chu, T. Nguyen, V. Pandey, Y. Zhou, H. N. Pham, R. Bar-Yoseph, S. Radom-Aizik, R. Jain, D. M. Cooper and M. Khine, "Respiration rate and volume measurements using wearable strain sensors" NPJ Digit. Med. **2** (1), 1-9 (2019).
39. K. Xu, Y. Fujita, Y. Lu, S. Honda, M. Shiomi, T. Arie, S. Akita and K. Takei, "A wearable body condition sensor system with wireless feedback alarm functions" Adv. Mater. **33** (18), 2008701 (2021).
40. A. Shahshahani, C. Laverdiere, S. Bhadra and Z. Zilic, "Ultrasound sensors for diaphragm motion tracking: An application in non-invasive respiratory monitoring" Sensors **18** (8), 2617 (2018).
41. A. Shahshahani, Z. Zilic and S. Bhadra, "Motion artifact reduction for respiratory monitoring: A multichannel ultrasound sensor for diaphragm tracking" IEEE Sens. J. **20** (13), 6872-6880 (2019).
42. J. Shin, B. Jeong, J. Kim, V. B. Nam, Y. Yoon, J. Jung, S. Hong, H. Lee, H. Eom and J. Yeo, "Sensitive wearable temperature sensor with seamless monolithic integration" Adv. Mater. **32** (2), 1905527 (2020).
43. S. Han, J. Kim, S. M. Won, Y. Ma, D. Kang, Z. Xie, K.-T. Lee, H. U. Chung, A. Banks and S. Min, "Battery-free, wireless sensors for full-body pressure and temperature mapping" Sci. Transl. Med. **10** (435), eaan4950 (2018).
44. H. Xu, W. Zheng, Y. Zhang, Y. Zhao, W. Wang, Y. Yuan, J. Zhang, Z. Huo, Y. Wang and N. Zhao, "A fully integrated, standalone stretchable device platform with in-sensor adaptive machine learning for rehabilitation" Preprint from Research Square, (2023). https://doi.org/10.21203/rs.3.rs-2671531/v1.
45. X. Ni, W. Ouyang, H. Jeong, J.-T. Kim, A. Tzavelis, A. Mirzazadeh, C. Wu, J. Y. Lee, M. Keller, C. K. Mummidisetty, M. Patel, N. Shawen, J. Huang, H. Chen, S. Ravi, J.-K. Chang, K. Lee, Y. Wu, F. Lie, Y. J. Kang, J. U. Kim, L. P. Chamorro, A. R. Banks, A. Bharat, A. Jayaraman,

S. Xu and J. A. Rogers, "Automated, multiparametric monitoring of respiratory biomarkers and vital signs in clinical and home settings for COVID-19 patients" Proc. Natl. Acad. Sci. U.S.A. **118** (19), e2026610118 (2021).
46. C. M. Alexander, L. E. Teller and J. B. Gross, "Principles of pulse oximetry: theoretical and practical considerations" Anesth. Analg. **68** (3), 368-376 (1989).
47. S. Shah, K. Majmudar, A. Stein, N. Gupta, S. Suppes, M. Karamanis, J. Capannari, S. Sethi and C. Patte, "Novel use of home pulse oximetry monitoring in COVID-19 patients discharged from the emergency department identifies need for hospitalization" Acad Emerg Med. **27** (8), 681-692 (2020).
48. F. Shaffer and J. P. Ginsberg, "An overview of heart rate variability metrics and norms" Front. Public Health. 258 (2017).
49. D. Kaliyaperumal, R. Karthikeyan, M. Alagesan and S. Ramalingam, "Characterization of cardiac autonomic function in COVID-19 using heart rate variability: a hospital based preliminary observational study" J. Basic Clin. Physiol. Pharmacol. **32** (3), 247-253 (2021).
50. M. B. Mol, M. T. Strous, F. H. van Osch, F. J. Vogelaar, D. G. Barten, M. Farchi, N. A. Foudraine and Y. Gidron, "Heart-rate-variability (HRV), predicts outcomes in COVID-19" PLoS One **16** (10), e0258841 (2021).
51. F. Hasty, G. García, H. Dávila, S. H. Wittels, S. Hendricks and S. Chong, "Heart rate variability as a possible predictive marker for acute inflammatory response in COVID-19 patients" Mil. Med. **186** (1-2), e34-e38 (2021).
52. A. Gracia-Perez-Bonfils, O. Martinez-Perez, E. Llurba and E. Chandraharan, "Fetal heart rate changes on the cardiotocograph trace secondary to maternal COVID-19 infection" Eur. J. Obstet. Gynecol. Reprod. Biol. **252**, 286-293 (2020).
53. T. Tamura, "Current progress of photoplethysmography and SPO2 for health monitoring" Biomed. Eng. Lett. **9** (1), 21-36 (2019).
54. M. Nitzan, A. Romem and R. Koppel, "Pulse oximetry: fundamentals and technology update" Med. Devices **7**, 231 (2014).
55. A. Gürün Kaya, M. Öz, I. Akdemir Kalkan, E. Gülten, G. Çınar, A. Azap and A. Kaya, "Is pulse oximeter a reliable tool for non-critically ill patients with COVID-19?" Int. J. Clin. Pract. **75** (12), e14983 (2021).
56. Y. Mendelson and C. Pujary, " Measurement site and photodetector size considerations in optimizing power consumption of a wearable reflectance pulse oximeter" presented at the Proceedings of the 25th Annual International Conference of the IEEE Engineering in Medicine and Biology Society (IEEE Cat. No. 03CH37439), 2003.
57. R. Wang, G. Blackburn, M. Desai, D. Phelan, L. Gillinov, P. Houghtaling and M. Gillinov, "Accuracy of wrist-worn heart rate monitors" JAMA Cardiol. **2** (1), 104-106 (2017).
58. A. Shcherbina, C. M. Mattsson, D. Waggott, H. Salisbury, J. W. Christle, T. Hastie, M. T. Wheeler and E. A. Ashley, "Accuracy in wrist-worn, sensor-based measurements of heart rate and energy expenditure in a diverse cohort" J. Pers. Med. **7** (2), 3 (2017).
59. S. Preejith, A. S. Ravindran, R. Hajare, J. Joseph and M. Sivaprakasam, " A wrist worn SpO 2 monitor with custom finger probe for motion artifact removal" presented at the 2016 38th Annual International Conference of the IEEE Engineering in Medicine and Biology Society (EMBC), 2016.
60. C. Phillips, D. Liaqat, M. Gabel and E. de Lara, " WristO2: Reliable Peripheral Oxygen Saturation Readings from Wrist-Worn Pulse Oximeters" presented at the 2021 IEEE International

Conference on Pervasive Computing and Communications Workshops and other Affiliated Events (PerCom Workshops), 2021.
61. B. Bent, B. A. Goldstein, W. A. Kibbe and J. P. Dunn, "Investigating sources of inaccuracy in wearable optical heart rate sensors" npj Digit. Med. **3** (1), 1-9 (2020).
62. D.-H. Kim, N. Lu, R. Ma, Y.-S. Kim, R.-H. Kim, S. Wang, J. Wu, S. M. Won, H. Tao, A. Islam, K. J. Yu, T.-i. Kim, R. Chowdhury, M. Ying, L. Xu, M. Li, H.-J. Chung, H. Keum, M. McCormick, P. Liu, Y.-W. Zhang, F. G. Omenetto, Y. Huang, T. Coleman and J. A. Rogers, "Epidermal electronics" Science **333** (6044), 838-843 (2011).
63. A. Y. Rwei, W. Lu, C. Wu, K. Human, E. Suen, D. Franklin, M. Fabiani, G. Gratton, Z. Xie and Y. Deng, "A wireless, skin-interfaced biosensor for cerebral hemodynamic monitoring in pediatric care" Proc. Natl. Acad. Sci. U.S.A. **117** (50), 31674-31684 (2020).
64. S. Cai, X. Xu, W. Yang, J. Chen and X. Fang, "Materials and designs for wearable photodetectors" Adv. Mater. **31** (18), 1808138 (2019).
65. H. Zhang and J. A. Rogers, "Recent advances in flexible inorganic light emitting diodes: From materials design to integrated optoelectronic platforms" Adv. Opt. Mater. **7** (2), 1800936 (2019).
66. P. C. Chow and T. Someya, "Organic photodetectors for next-generation wearable electronics" Adv. Mater. **32** (15), 1902045 (2020).
67. G. Lu, F. Yang, J. Taylor and J. Stein, "A comparison of photoplethysmography and ECG recording to analyse heart rate variability in healthy subjects" J. Med. Eng. Technol **33** (8), 634-641 (2009).
68. H. C. Ates, A. K. Yetisen, F. Güder and C. Dincer, "Wearable devices for the detection of COVID-19" Nat. Electron. **4** (1), 13-14 (2021).
69. T. Yokota, P. Zalar, M. Kaltenbrunner, H. Jinno, N. Matsuhisa, H. Kitanosako, Y. Tachibana, W. Yukita, M. Koizumi and T. Someya, "Ultraflexible organic photonic skin" Sci. Adv. **2** (4), e1501856 (2016).
70. H. Lee, E. Kim, Y. Lee, H. Kim, J. Lee, M. Kim, H.-J. Yoo and S. Yoo, "Toward all-day wearable health monitoring: An ultralow-power, reflective organic pulse oximetry sensing patch" Sci. Adv. **4** (11), eaas9530 (2018).
71. Y. Khan, D. Han, A. Pierre, J. Ting, X. Wang, C. M. Lochner, G. Bovo, N. Yaacobi-Gross, C. Newsome, R. Wilson and A. C. Arias, "A flexible organic reflectance oximeter array" Proc. Natl. Acad. Sci. U.S.A. **115** (47), E11015-E11024 (2018).
72. Y. Khan, D. Han, J. Ting, M. Ahmed, R. Nagisetty and A. C. Arias, "Organic multi-channel optoelectronic sensors for wearable health monitoring" IEEE Access **7**, 128114-128124 (2019).
73. J. Kim, P. Gutruf, A. M. Chiarelli, S. Y. Heo, K. Cho, Z. Xie, A. Banks, S. Han, K. I. Jang, J. W. Lee, K.-T. Lee, X. Fen, Y. Huan, M. Fabiani, G. Gratton, U. Paik and J. A. Rogers, "Miniaturized battery-free wireless systems for wearable pulse oximetry" Adv. Funct. Mater. **27** (1), 1604373 (2017).
74. H. U. Chung, B. H. Kim, J. Y. Lee, J. Lee, Z. Xie, E. M. Ibler, K. Lee, A. Banks, J. Y. Jeong, J. Kim, C. Ogle, D. Grande, Y. Yu, H. Jang, P. Assem, D. Ryu, J. W. Kwak, M. Namkoong, J. B. Park, Y. Lee, D. H. Kim, A. Ryu, J. Jeong, K. You, B. Ji, Z. Liu, Q. Huo, X. Feng, Y. Deng, Y. Xu, Kyung-InJang, J. Kim, Y. Zhang, R. Ghaffar, C. Rand, M. Schau, A. Hamvas, D. E. Weese-Mayer, Y. Huang, S. M. Lee, C. H. Lee, N. R. Shanbhag, A. S. Palle, S. Xu and J. A. Rogers, "Binodal, wireless epidermal electronic systems with in-sensor analytics for neonatal intensive care" Science **363** (6430), eaau0780 (2019).
75. C.-J. Lim and J.-W. Park, "Wearable transcutaneous oxygen sensor for health monitoring" Sens. Actuator A Phys. **298**, 111607 (2019).

76. S. Abdollahi, E. J. Markvicka, C. Majidi and A. W. J. A. h. m. Feinberg, "3D Printing Silicone Elastomer for Patient-Specific Wearable Pulse Oximeter" Adv. Healthc. Mater.**9** (15), 1901735 (2020).
77. D. Han, Y. Khan, J. Ting, J. Zhu, C. Combe, A. Wadsworth, I. McCulloch and A. C. Arias, "Pulse oximetry using organic optoelectronics under ambient light" Adv. Mater. Technol. **5** (5), 1901122 (2020).
78. S.-H. Bae, D. Kim, S.-Y. Chang, J. Hur, H. Kim, J.-W. Lee, B. Zhu, T.-H. Han, C. Choi, D. L. Huffaker, D. D. Carlo, Y. Yang and Y. S. Rim, "Hybrid integrated photomedical devices for wearable vital sign tracking" ACS Sens. **5** (6), 1582-1588 (2020).
79. M. Xu and L. V. Wang, "Photoacoustic imaging in biomedicine" Rev. Sci. Instrum. **77** (4), 041101 (2006).
80. L. V. Wang and S. Hu, "Photoacoustic tomography: in vivo imaging from organelles to organs" science **335** (6075), 1458-1462 (2012).
81. M. Li, Y. Tang and J. Yao, "Photoacoustic tomography of blood oxygenation: a mini review" Photoacoustics **10**, 65-73 (2018).
82. R. Bulsink, M. Kuniyil Ajith Singh, M. Xavierselvan, S. Mallidi, W. Steenbergen and K. J. Francis, "Oxygen saturation imaging using LED-based photoacoustic system" Sensors **21** (1), 283 (2021).
83. X. Gao, X. Chen, H. Hu, X. Wang, W. Yue, J. Mu, Z. Lou, R. Zhang, K. Shi and X. Chen, "A photoacoustic patch for three-dimensional imaging of hemoglobin and core temperature" Nat. Commun. **13** (1), 1-13 (2022).
84. J. Dunn, L. Kidzinski, R. Runge, D. Witt, J. L. Hicks, S. M. Schüssler-Fiorenza Rose, X. Li, A. Bahmani, S. L. Delp, T. Hastie and M. P. Snyder, "Wearable sensors enable personalized predictions of clinical laboratory measurements" Nat. Med. **27** (6), 1105-1112 (2021).
85. S. Ryu, P. Lee, J. B. Chou, R. Xu, R. Zhao, A. J. Hart and S.-G. Kim, "Extremely elastic wearable carbon nanotube fiber strain sensor for monitoring of human motion" ACS Nano **9** (6), 5929-5936 (2015).
86. C. Wang, X. Li, H. Hu, L. Zhang, Z. Huang, M. Lin, Z. Zhang, Z. Yin, B. Huang, H. Gong, S. Bhaskaran, Y. Gu, M. Makihata, Y. Guo, Y. Lei, Y. Chen, C. Wang, Y. Li, T. Zhang, Z. Chen, A. P. Pisano, L. Zhang, Q. Zhou and S. Xu, "Monitoring of the central blood pressure waveform via a conformal ultrasonic device" Nat. Biomed. Eng **2** (9), 687-695 (2018).
87. T. Q. Trung, S. Ramasundaram, B. U. Hwang and N. E. Lee, "An all-elastomeric transparent and stretchable temperature sensor for body-attachable wearable electronics" Adv. Mater. **28** (3), 502-509 (2016).
88. T. Kim, J. Park, J. Sohn, D. Cho and S. Jeon, "Bioinspired, highly stretchable, and conductive dry adhesives based on 1D–2D hybrid carbon nanocomposites for all-in-one ECG electrodes" ACS Nano **10** (4), 4770-4778 (2016).
89. J. Min, J. R. Sempionatto, H. Teymourian, J. Wang and W. Gao, "Wearable electrochemical biosensors in North America" Biosens. Bioelectron. **172**, 112750 (2021).
90. Z. Wang, Z. Hao, X. Wang, C. Huang, Q. Lin, X. Zhao and Y. Pan, "A flexible and regenerative aptameric graphene–Nafion biosensor for cytokine storm biomarker monitoring in undiluted biofluids toward wearable applications" Adv. Funct. Mater. **31** (4), 2005958 (2021).
91. Z. Hao, Y. Luo, C. Huang, Z. Wang, G. Song, Y. Pan, X. Zhao and S. Liu, "An Intelligent Graphene-Based Biosensing Device for Cytokine Storm Syndrome Biomarkers Detection in Human Biofluids" Small **17** (29), 2101508 (2021).

92. R. M. Torrente-Rodríguez, H. Lukas, J. Tu, J. Min, Y. Yang, C. Xu, H. B. Rossiter and W. Gao, "SARS-CoV-2 RapidPlex: a graphene-based multiplexed telemedicine platform for rapid and low-cost COVID-19 diagnosis and monitoring" Matter **3** (6), 1981-1998 (2020).
93. T. Tan, B. Khoo, E. G. Mills, M. Phylactou, B. Patel, P. C. Eng, L. Thurston, B. Muzi, K. Meeran, A. T. Prevost, A. N. Comninos, A. Abbara and W. S. Dhillo, "Association between high serum total cortisol concentrations and mortality from COVID-19" Lancet Diabetes Endocrinol. **8** (8), 659-660 (2020).
94. Y. Zheng, R. Omar, R. Zhang, N. Tang, M. Khatib, Q. Xu, Y. Milyutin, W. Saliba, Y. Y. Broza, W. Wu, M. Yuan and H. Haick, "A Wearable Microneedle-Based Extended Gate Transistor for Real-Time Detection of Sodium in Interstitial Fluids" Adv. Mater. **34** (10), 2108607 (2022).
95. S. Montazersaheb, S. M. Hosseiniyan Khatibi, M. S. Hejazi, V. Tarhriz, A. Farjami, F. Ghasemian Sorbeni, R. Farahzadi and T. Ghasemnejad, "COVID-19 infection: an overview on cytokine storm and related interventions" Virol. J. **19** (1), 1-15 (2022).
96. S. Hojyo, M. Uchida, K. Tanaka, R. Hasebe, Y. Tanaka, M. Murakami and T. Hirano, "How COVID-19 induces cytokine storm with high mortality" Inflamm. Regen. **40** (1), 1-7 (2020).
97. X. Chen, B. Zhao, Y. Qu, Y. Chen, J. Xiong, Y. Feng, D. Men, Q. Huang, Y. Liu, B. Yang, J. Ding and F. Li, "Detectable serum SARS-CoV-2 viral load (RNAaemia) is closely correlated with drastically elevated interleukin 6 (IL-6) level in critically ill COVID-19 patients" Clin. Infect. Dis. (2020).
98. C. Huang, Y. Wang, X. Li, L. Ren, J. Zhao, Y. Hu, L. Zhang, G. Fan, J. Xu, X. Gu, Z. Cheng, T. Yu, J. Xia, Y. Wei, W. Wu, X. Xie, W. Yin, H. Li, M. Liu, Y. Xiao, H. Gao, L. Guo, J. Xie, G. Wang, R. Jiang, Z. Gao, Q. Jin, J. Wang and B. Cao, "Clinical features of patients infected with 2019 novel coronavirus in Wuhan, China" Lancet **395** (10223), 497-506 (2020).
99. J. Liu, S. Li, J. Liu, B. Liang, X. Wang, H. Wang, W. Li, Q. Tong, J. Yi, L. Zhao, L. Xiong, C. Guo, J. Tian, J. Luo, J. Yao, R. Pang, H. Shen, C. Peng, T. Liu, Q. Zhang, J. Wu, L. Xu, S. Lu, B. Wang, Z. Weng, C. Han, H. Zhu, R. Zhou, H. Zhou, X. Chen, P. Ye, B. Zhu, L. Wang, W. Zhou, S. He, Y. He, S. Jie, P. Wei, J. Zhang, Y. Lu, W. Wang, L. Zhang, L. Li, F. Zhou, J. Wang, U. Dittmer, M. Lu, Y. Hu, D. Yang and X. Zheng, "Longitudinal characteristics of lymphocyte responses and cytokine profiles in the peripheral blood of SARS-CoV-2 infected patients" EBioMedicine **55**, 102763 (2020).
100. T. Liu, J. Zhang, Y. Yang, H. Ma, Z. Li, J. Zhang, J. Cheng, X. Zhang, Y. Zhao, Z. Xia, L. Zhang, G. Wu and J. Yi, "The potential role of IL-6 in monitoring coronavirus disease 2019" medRXiv **3548761**, 2020 (2020).
101. D. Wang, B. Hu, C. Hu, F. Zhu, X. Liu, J. Zhang, B. Wang, H. Xiang, Z. Cheng, Y. Xiong, Y. Zhao, Y. Li, X. Wang and Z. Peng, "Clinical characteristics of 138 hospitalized patients with 2019 novel coronavirus–infected pneumonia in Wuhan, China" JAMA **323** (11), 1061-1069 (2020).
102. M. Rahmati and M. A. Moosavi, "Cytokine-targeted therapy in severely ill COVID-19 patients: options and cautions" EJMA **4** (2), 179-181 (2020).
103. O. Parlak, S. T. Keene, A. Marais, V. F. Curto and A. Salleo, "Molecularly selective nanoporous membrane-based wearable organic electrochemical device for noninvasive cortisol sensing" Sci. Adv. **4** (7), eaar2904 (2018).
104. R. M. Torrente-Rodríguez, J. Tu, Y. Yang, J. Min, M. Wang, Y. Song, Y. Yu, C. Xu, C. Ye, W. W. IsHak and W. Gao, "Investigation of cortisol dynamics in human sweat using a graphene-based wireless mHealth system" Matter **2** (4), 921-937 (2020).

105. B. Wang, C. Zhao, Z. Wang, K.-A. Yang, X. Cheng, W. Liu, W. Yu, S. Lin, Y. Zhao, K. M. Cheung, H. Lin, H. Hojaiji, P. S. Weiss, M. N. Stojanović, A. J. Tomiyama, A. M. Andrews and S. Emaminejad, "Wearable aptamer-field-effect transistor sensing system for noninvasive cortisol monitoring" Sci. Adv. **8** (1), eabk0967 (2022).
106. H. Li, G. Wu, Z. Weng, H. Sun, R. Nistala and Y. Zhang, "Microneedle-Based Potentiometric Sensing System for Continuous Monitoring of Multiple Electrolytes in Skin Interstitial Fluids" ACS Sens. **6** (6), 2181-2190 (2021).
107. V. Thiviyanathan and D. G. Gorenstein, "Aptamers and the next generation of diagnostic reagents" Proteomics Clin Appl. **6** (11-12), 563-573 (2012).
108. C. Han, C. Duan, S. Zhang, B. Spiegel, H. Shi, W. Wang, L. Zhang, R. Lin, J. Liu, Z. Ding and X. Hou, "Digestive symptoms in COVID-19 patients with mild disease severity: clinical presentation, stool viral RNA testing, and outcomes" Am. J. Gastroenterol. (2020).
109. A. J. Bandodkar, W. J. Jeang, R. Ghaffari and J. A. Rogers, "Wearable sensors for biochemical sweat analysis" Annu. Rev. Anal. Chem **12** (1), 1-22 (2019).
110. A. J. Bandodkar, P. Gutruf, J. Choi, K. Lee, Y. Sekine, J. T. Reeder, W. J. Jeang, A. J. Aranyosi, S. P. Lee, J. B. Model, R. Ghaffari, C.-J. Su, J. P. Leshock, T. Ray, A. Verrillo, K. Thomas, V. Krishnamurthi, S. Han, J. Kim, S. Krishnan, T. Hang and J. A. Rogers, "Battery-free, skin-interfaced microfluidic/electronic systems for simultaneous electrochemical, colorimetric, and volumetric analysis of sweat" Sci. Adv. **5** (1), eaav3294 (2019).
111. K. Y. Goud, C. Moonla, R. K. Mishra, C. Yu, R. Narayan, I. Litvan and J. Wang, "Wearable electrochemical microneedle sensor for continuous monitoring of levodopa: toward Parkinson management" ACS Sens. **4** (8), 2196-2204 (2019).
112. M. Parrilla, M. Cuartero, S. Padrell Sánchez, M. Rajabi, N. Roxhed, F. Niklaus and G. n. A. Crespo, "Wearable all-solid-state potentiometric microneedle patch for intradermal potassium detection" Anal. Chem. **91** (2), 1578-1586 (2018).
113. Z. Wang, J. Luan, A. Seth, L. Liu, M. You, P. Gupta, P. Rathi, Y. Wang, S. Cao, Q. Jiang, X. Zhang, R. Gupta, Q. Zhou, J. J. Morrissey, E. L. Scheller, J. S. Rudra and S. Singamaneni, "Microneedle patch for the ultrasensitive quantification of protein biomarkers in interstitial fluid" Nat. Biomed. Eng. **5** (1), 64-76 (2021).
114. W. Gao, S. Emaminejad, H. Y. Y. Nyein, S. Challa, K. Chen, A. Peck, H. M. Fahad, H. Ota, H. Shiraki and D. Kiriya, "Fully integrated wearable sensor arrays for multiplexed in situ perspiration analysis" Nature **529** (7587), 509-514 (2016).
115. G. Quer, J. M. Radin, M. Gadaleta, K. Baca-Motes, L. Ariniello, E. Ramos, V. Kheterpal, E. J. Topol and S. R. Steinhubl, "Wearable sensor data and self-reported symptoms for COVID-19 detection" Nat. Med. **27** (1), 73-77 (2021).
116. B. Shan, Y. Y. Broza, W. Li, Y. Wang, S. Wu, Z. Liu, J. Wang, S. Gui, L. Wang, Z. Zhang, W. Liu, S. Zhou, W. Jin, Q. Zhang, D. Hu, L. Lin, Q. Zhang, W. Li, J. Wang, H. Liu, Y. Pan and H. Haick, "Multiplexed nanomaterial-based sensor array for detection of COVID-19 in exhaled breath" ACS nano **14** (9), 12125-12132 (2020).
117. L. Rui, S. Chen, K. Ho, M. Rantz and M. Skubic, "Estimation of human walking speed by Doppler radar for elderly care" J. Ambient Intell. Smart Environ **9** (2), 181-191 (2017).
118. K. T. Tanweer, S. R. Hasan and A. M. Kamboh, " Motion artifact reduction from PPG signals during intense exercise using filtered X-LMS" presented at the 2017 IEEE international symposium on circuits and systems (ISCAS), 2017.

119. Z. Zhang, Z. Pi and B. Liu, "TROIKA: A general framework for heart rate monitoring using wrist-type photoplethysmographic signals during intensive physical exercise" IEEE. Trans. Biomed. Eng. **62** (2), 522-531 (2014).
120. R. Yousefi, M. Nourani, S. Ostadabbas and I. Panahi, "A motion-tolerant adaptive algorithm for wearable photoplethysmographic biosensors" IEEE J Biomed Health Inform **18** (2), 670-681 (2013).
121. D. Bian, P. Mehta and N. Selvaraj, " Respiratory Rate Estimation using PPG: A Deep Learning Approach" presented at the 2020 42nd annual international conference of the IEEE engineering in Medicine & Biology Society (EMBC), 2020.
122. Y. Cho, S. J. Julier, N. Marquardt and N. Bianchi-Berthouze, "Robust tracking of respiratory rate in high-dynamic range scenes using mobile thermal imaging" Biomed. Opt. Express **8** (10), 4480-4503 (2017).
123. H. Wu, W. Ruan, J. Wang, D. Zheng, B. Liu, Y. Geng, X. Chai, J. Chen, K. Li, S. Li and S. Helal, "Interpretable machine learning for covid-19: An empirical study on severity prediction task" IEEE Trans Artif Intell. (2021).
124. A. Dairi, F. Harrou and Y. Sun, "Deep generative learning-based 1-svm detectors for unsupervised covid-19 infection detection using blood tests" IEEE Trans. Instrum. Meas. **71**, 1-11 (2021).
125. R. a. Mohammedqasem, H. Mohammedqasim and O. Ata, "Real-time data of COVID-19 detection with IoT sensor tracking using artificial neural network" Comput. Electr. Eng. **100**, 107971 (2022).
126. M. Otoom, N. Otoum, M. A. Alzubaidi, Y. Etoom and R. Banihani, "An IoT-based framework for early identification and monitoring of COVID-19 cases" Biomed. Signal Process. Control. **62**, 102149 (2020).
127. Y. Gao, G.-Y. Cai, W. Fang, H.-Y. Li, S.-Y. Wang, L. Chen, Y. Yu, D. Liu, S. Xu, P.-F. Cui, S.-Q. Zeng, X.-X. Feng, R.-D. Yu, Y. Wang, Y. Yuan, X.-F. Jiao, J.-H. Chi, J.-H. Liu, R.-Y. Li, X. Zheng, C.-Y. Song, N. Jin, W.-J. Gong, X.-Y. Liu, L. Huang, X. Tian, L. Li, H. Xing, D. Ma, C.-R. Li, F. Ye and Q.-L. Gao, "Machine learning based early warning system enables accurate mortality risk prediction for COVID-19" Nat. Commun. **11** (1), 1-10 (2020).
128. B. Shen, X. Yi, Y. Sun, X. Bi, J. Du, C. Zhang, S. Quan, F. Zhang, R. Sun, L. Qian, W. Ge, W. Liu, S. Liang, H. Chen, Y. Zhang, J. Li, J. Xu, Z. He, B. Chen, J. Wang, H. Yan, Y. Zheng, D. Wang, J. Zhu, Z. Kong, Z. Kang, X. Liang, X. Ding, G. Ruan, N. Xiang, X. Cai, H. Gao, L. Li, S. Li, Q. Xiao, T. Lu, Y. Zhu, H. Liu, H. Chen and T. Guo, "Proteomic and metabolomic characterization of COVID-19 patient sera" Cell **182** (1), 59-72. e15 (2020).
129. Y. Xiong, Y. Ma, L. Ruan, D. Li, C. Lu and L. Huang, "Comparing different machine learning techniques for predicting COVID-19 severity" Infect. Dis. Poverty **11** (1), 1-9 (2022).
130. D. M. Del Valle, S. Kim-Schulze, H.-H. Huang, N. D. Beckmann, S. Nirenberg, B. Wang, Y. Lavin, T. H. Swartz, D. Madduri, A. Stock, T. U. Marron, H. Xie, M. Patel, K. Tuballes, O. V. Oekelen, A. Rahman, P. Kovatch, J. A. Aberg, E. Schadt, S. Jagannath, M. Mazumdar, A. W. Charney, A. Firpo-Betancourt, D. R. Mend, J. Jhang, D. Reich, K. Sigel, C. Cordon-Cardo, M. Feldmann, S. Parekh, M. Merad and S. Gnjatic, "An inflammatory cytokine signature predicts COVID-19 severity and survival" Nat. Med. **26** (10), 1636-1643 (2020).
131. H. Mohammedqasim and O. Ata, "Real-time data of COVID-19 detection with IoT sensor tracking using artificial neural network" Comput. Electr. Eng. **100**, 107971 (2022).
132. Q. Yang, J. Li, Z. Zhang, X. Wu, T. Liao, S. Yu, Z. You, X. Hou, J. Ye, G. Liu, S. Ma, G. Xie, Y. Zhou, M. Li, M. Wu, Y. Feng, W. Wang, L. Li, D. Xie, Y. Hu, X. Liu, B. Wang, S. Zhao,

L. Li, C. Luo, T. Tang, H. Wu, T. Hu, G. Yang, B. Luo, L. Li, X. Yang, Q. Li, Z. Xu, H. Wu and J. Sun, "Clinical characteristics and a decision tree model to predict death outcome in severe COVID-19 patients" BMC Infect. Dis. **21** (1), 1-9 (2021).
133. C. M. Yeşilkanat, "Spatio-temporal estimation of the daily cases of COVID-19 in worldwide using random forest machine learning algorithm" Chaos Solit. Fractals. **140**, 110210 (2020).
134. V. A. d. F. Barbosa, J. C. Gomes, M. A. de Santana, C. L. de Lima, R. B. Calado, C. R. Bertoldo Junior, J. E. d. A. Albuquerque, R. G. de Souza, R. J. E. de Araújo, L. A. R. Mattos Junior, R. E. d. Souza and W. P. D. Santos, "Covid-19 rapid test by combining a random forest-based web system and blood tests" J. Biomol. Struct. Dyn., 1-20 (2021).
135. B. Shi, H. Ye, J. Zheng, Y. Zhu, A. A. Heidari, L. Zheng, H. Chen, L. Wang and P. Wu, "Early recognition and discrimination of covid-19 severity using slime mould support vector machine for medical decision-making" IEEE Access **9**, 121996-122015 (2021).
136. T. B. Alakus and I. Turkoglu, "Comparison of deep learning approaches to predict COVID-19 infection" Chaos Solit. Fractals **140**, 110120 (2020).
137. ANNE One sensor https://www.sibelhealth.com/anne-one.
138. Z. Gong, P. Zhong and W. Hu, "Diversity in machine learning" IEEE Access **7**, 64323-64350 (2019).
139. S. Imani, A. J. Bandodkar, A. Mohan, R. Kumar, S. Yu, J. Wang and P. P. Mercier, "A wearable chemical–electrophysiological hybrid biosensing system for real-time health and fitness monitoring" Nat. Commun. **7** (1), 1-7 (2016).
140. L. D. Blackman, P. A. Gunatillake, P. Cass and K. E. Locock, "An introduction to zwitterionic polymer behavior and applications in solution and at surfaces" Chem. Soc. Rev. **48** (3), 757-770 (2019).
141. D. Chan, J. C. Chien, E. Axpe, L. Blankemeier, S. W. Baker, S. Swaminathan, V. A. Piunova, D. Y. Zubarev, C. L. Maikawa, A. K. Grosskopf, J. L. Mann, H. T. Soh and E. A. Appel, "Combinatorial polyacrylamide hydrogels for preventing biofouling on implantable biosensors" Adv. Mater., 2109764 (2022).
142. A. Koh, D. Kang, Y. Xue, S. Lee, R. M. Pielak, J. Kim, T. Hwang, S. Min, A. Banks, P. Bastien, M. C. Manco, L. Wang, K. R. Ammann, K.-I. Jang, P. Won, S. Han, R. Ghaffari, U. Paik, M. J. Slepian, G. Balooch, Y. Huang and J. A. Rogers, "A soft, wearable microfluidic device for the capture, storage, and colorimetric sensing of sweat" Sci. Transl. Med. **8** (366), 366ra165-366ra165 (2016).
143. A. Bandodkar, S. Lee, I. Huang, W. Li, S. Wang, C.-J. Su, W. Jeang, T. Hang, S. Mehta, N. Nyberg, P. Gutruf, J. Choi, J. Koo, J. T. Reeder, R. Tseng, R. Ghaffari and J. A. Rogers, "Sweat-activated biocompatible batteries for epidermal electronic and microfluidic systems" Nat. Electron. **3** (9), 554-562 (2020).
144. J. Heikenfeld, A. Jajack, B. Feldman, S. W. Granger, S. Gaitonde, G. Begtrup and B. A. Katchman, "Accessing analytes in biofluids for peripheral biochemical monitoring" Nat. Biotechnol **37** (4), 407-419 (2019).
145. J. W. Kim, S.-M. Moon, S.-u. Kang and B. Jang, "Effective privacy-preserving collection of health data from a user's wearable device" Appl. Sci. **10** (18), 6396 (2020).
146. C. Kang, H. Jung and Y. Lee, " Towards machine learning with zero real-world data" presented at the The 5th ACM Workshop on Wearable Systems and Applications, 2019.

PLEASE CITE THIS ARTICLE AS DOI: 10.1063/5.0140900

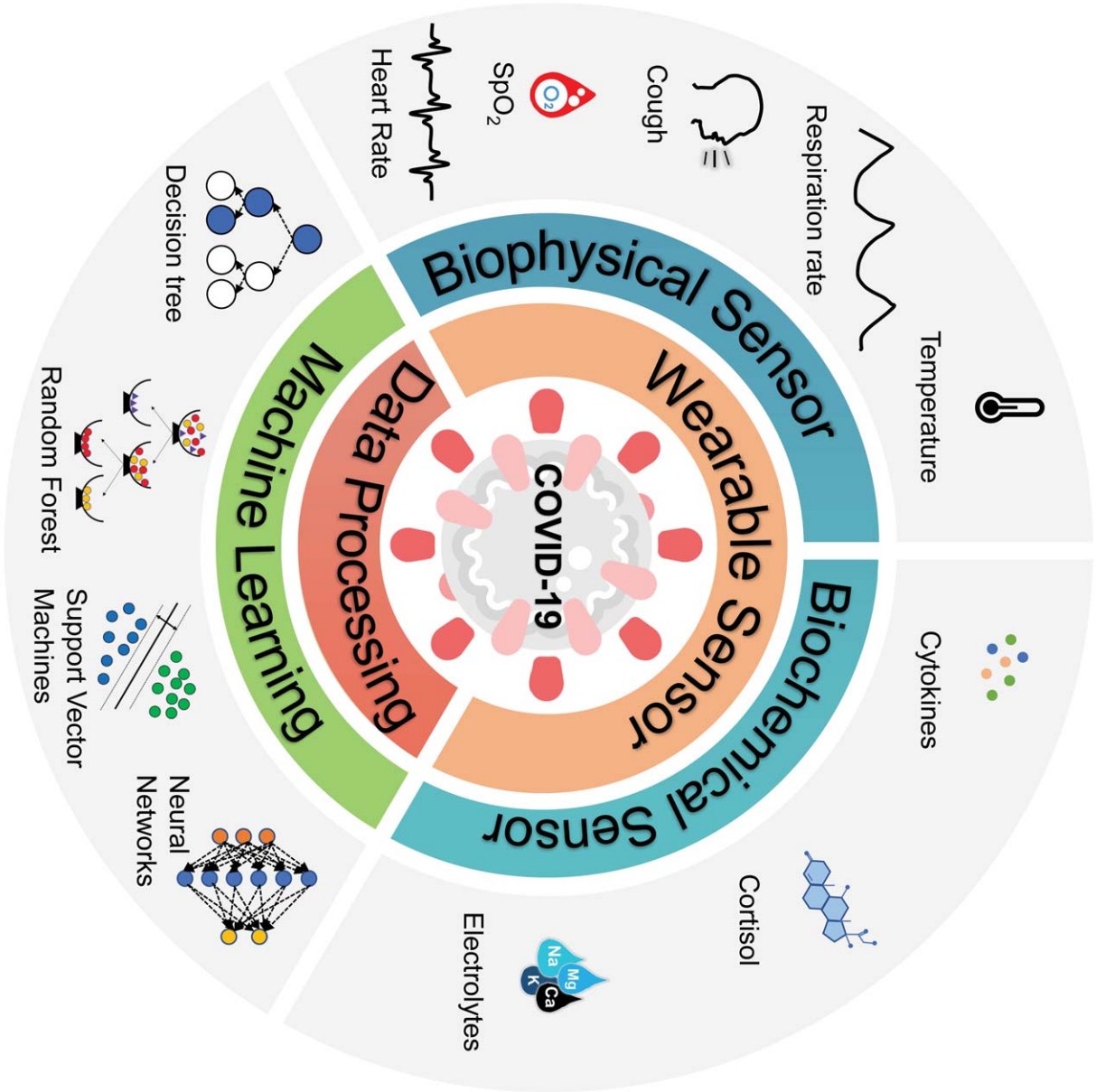

PLEASE CITE THIS ARTICLE AS DOI: 10.1063/5.0140900

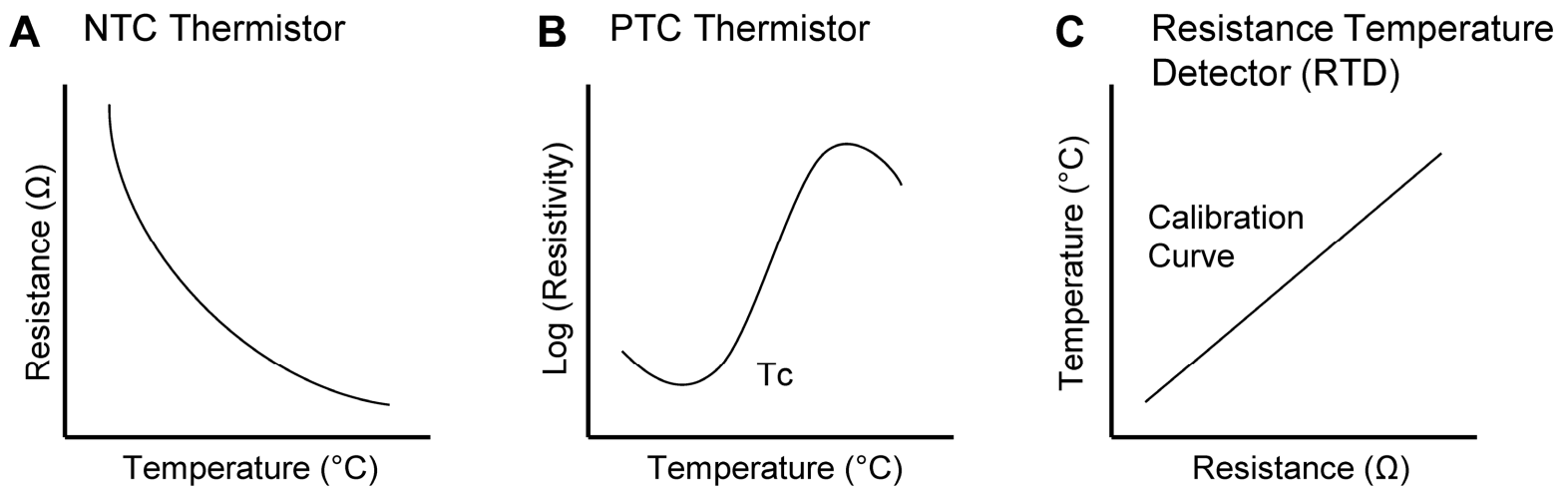

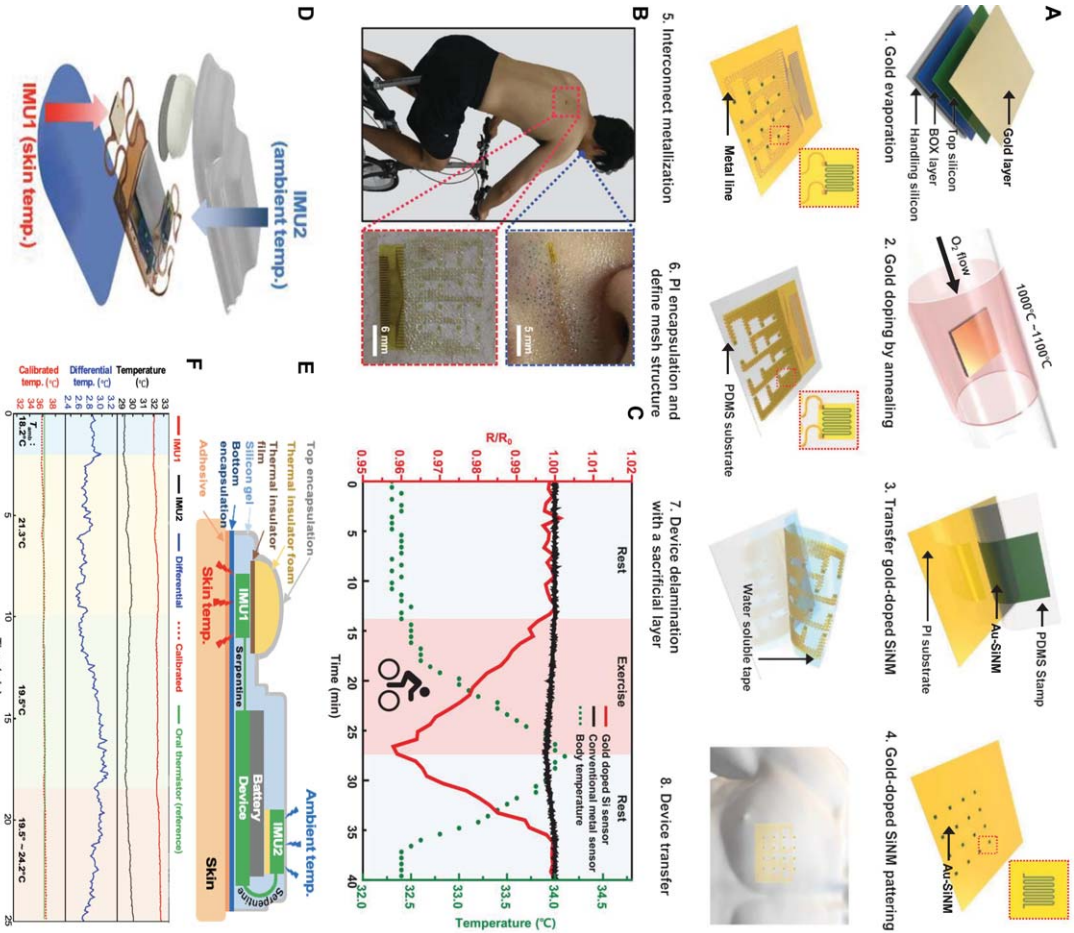

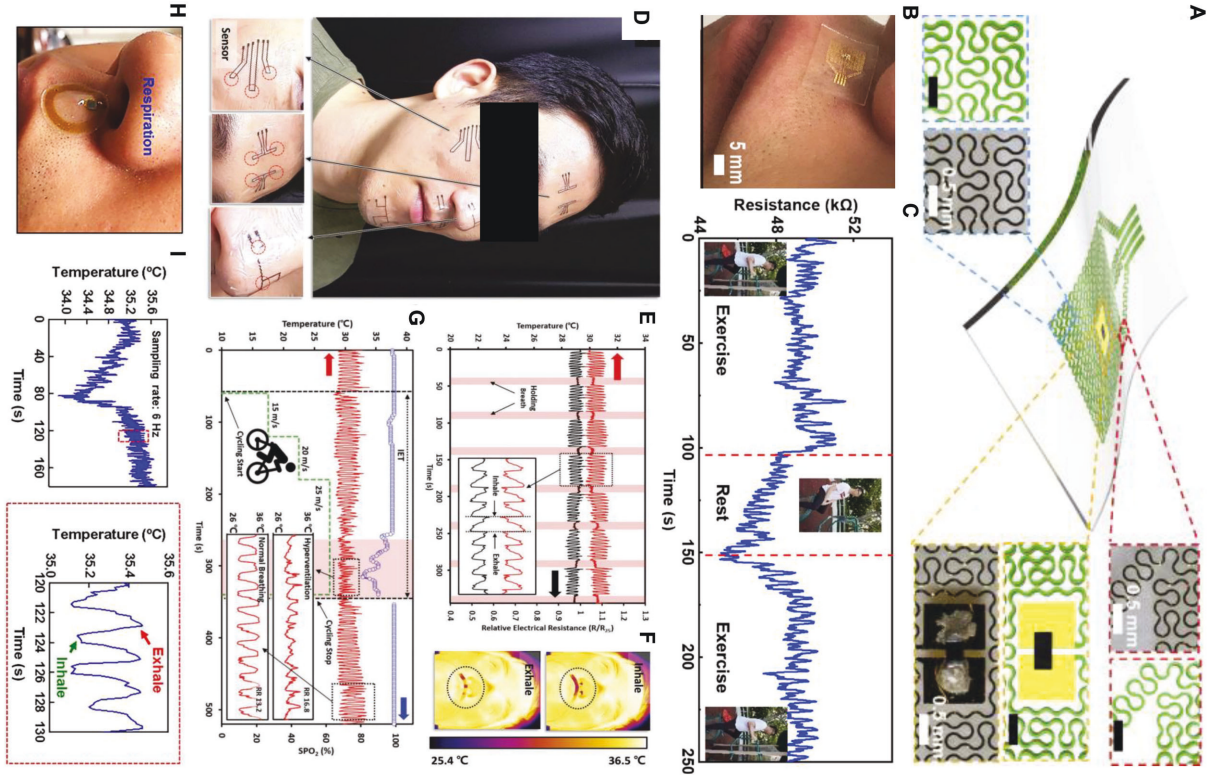

PLEASE CITE THIS ARTICLE AS DOI: 10.1063/5.0140900

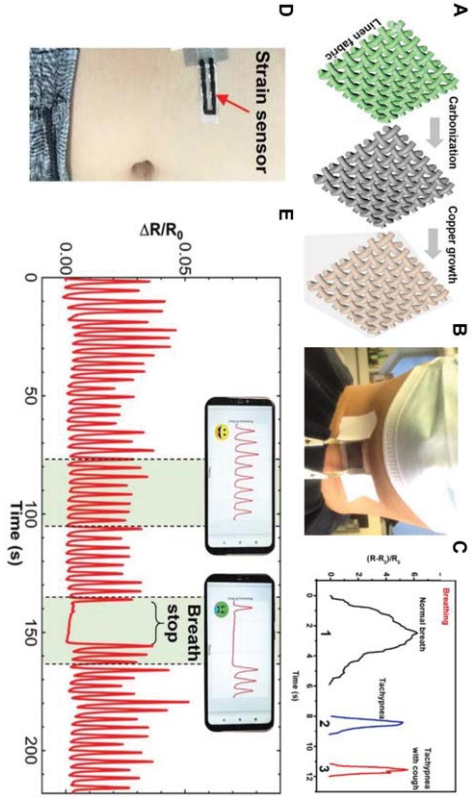

Biophysics Reviews

AIP Publishing

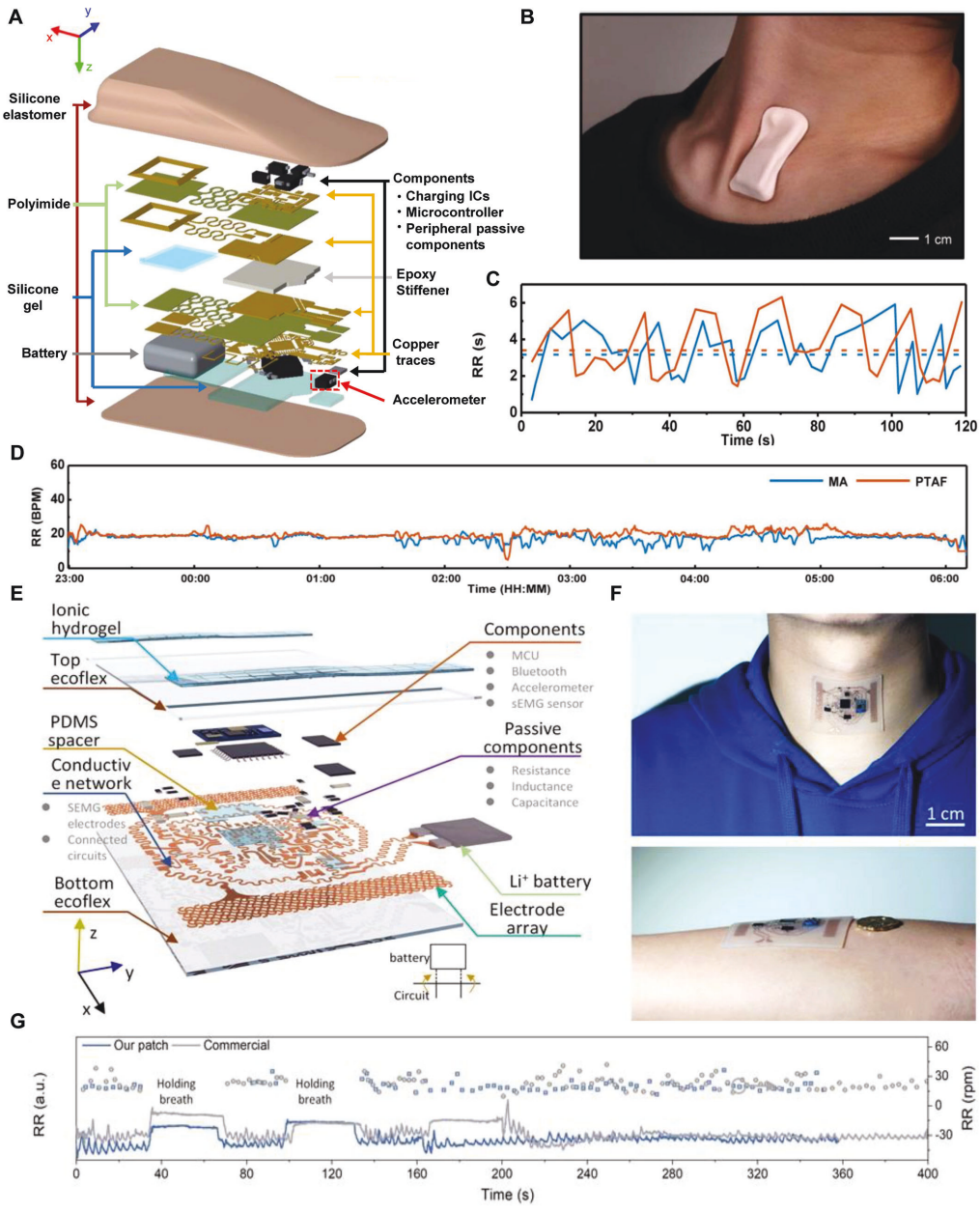

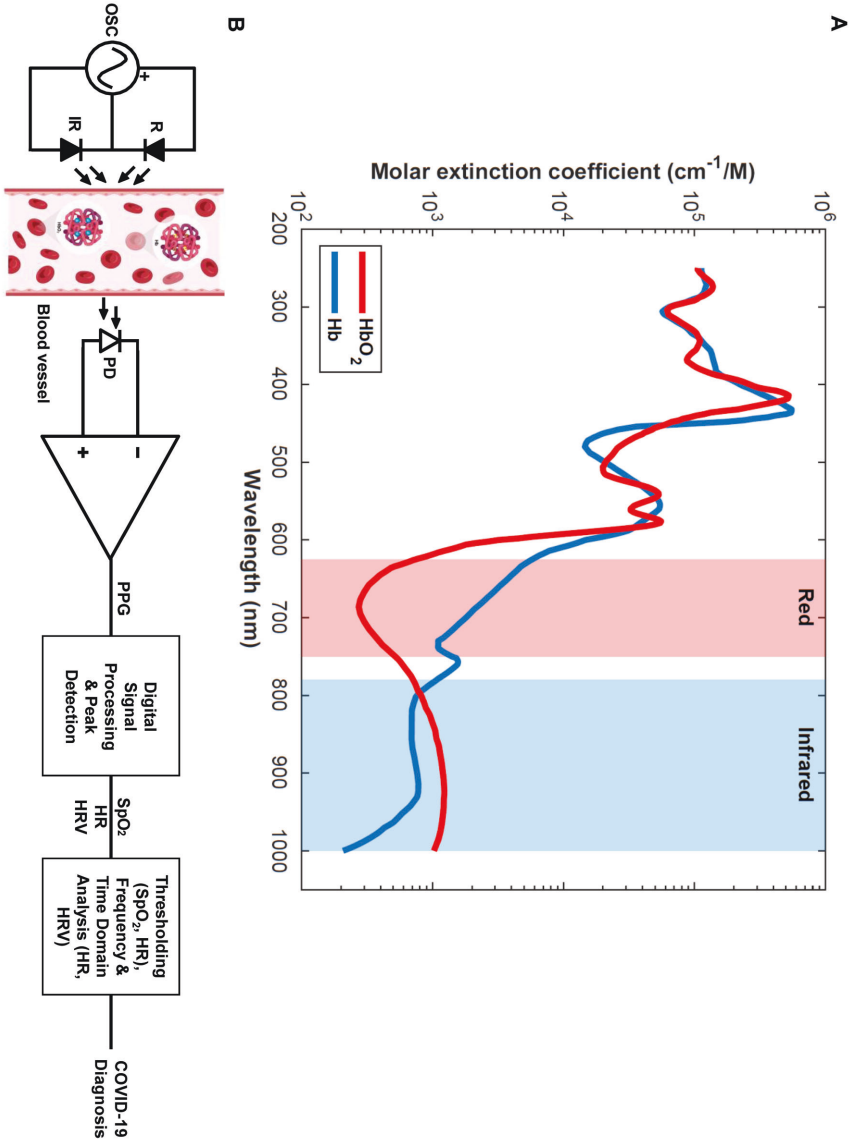

PLEASE CITE THIS ARTICLE AS DOI: 10.1063/5.0140900

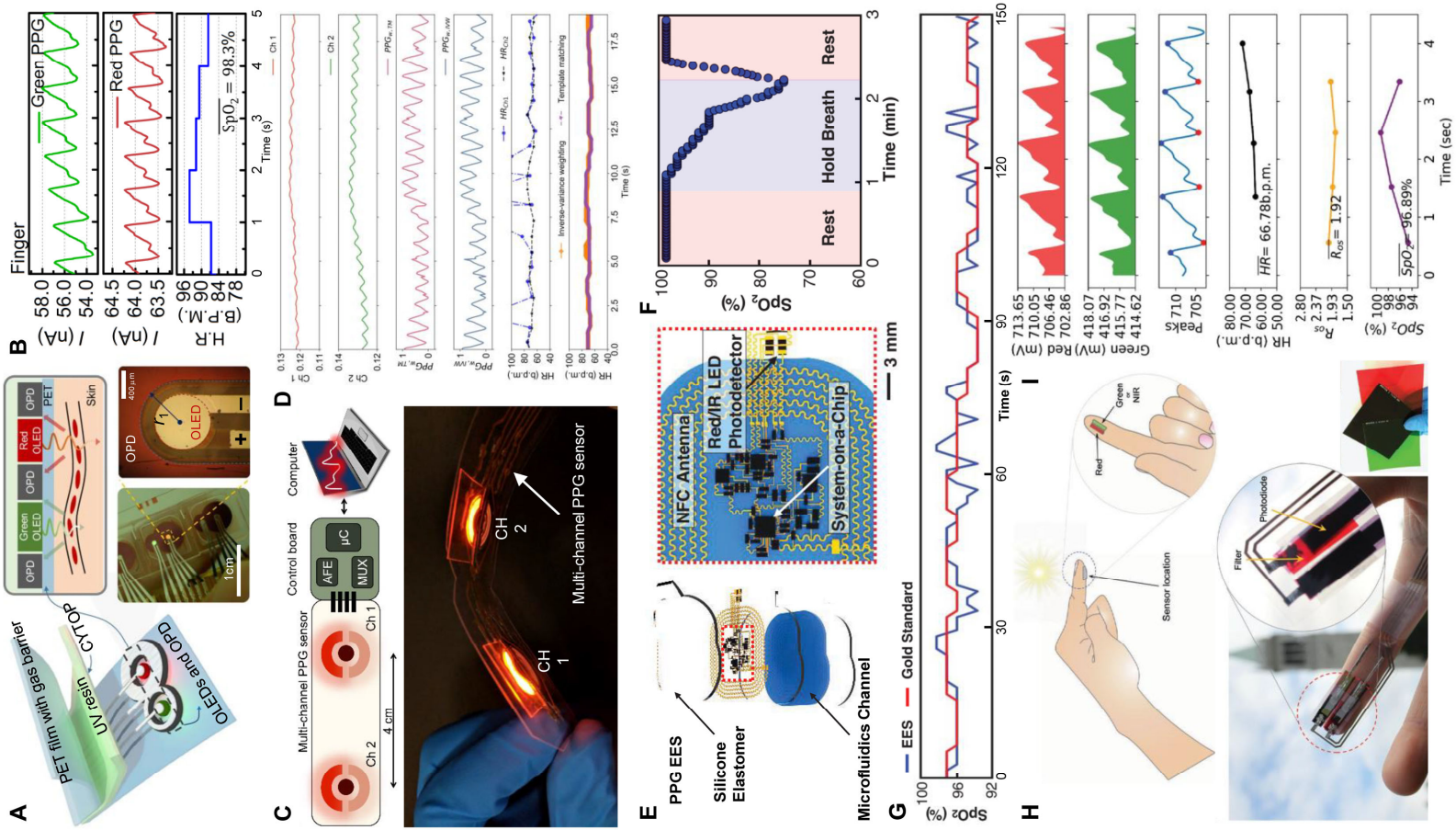

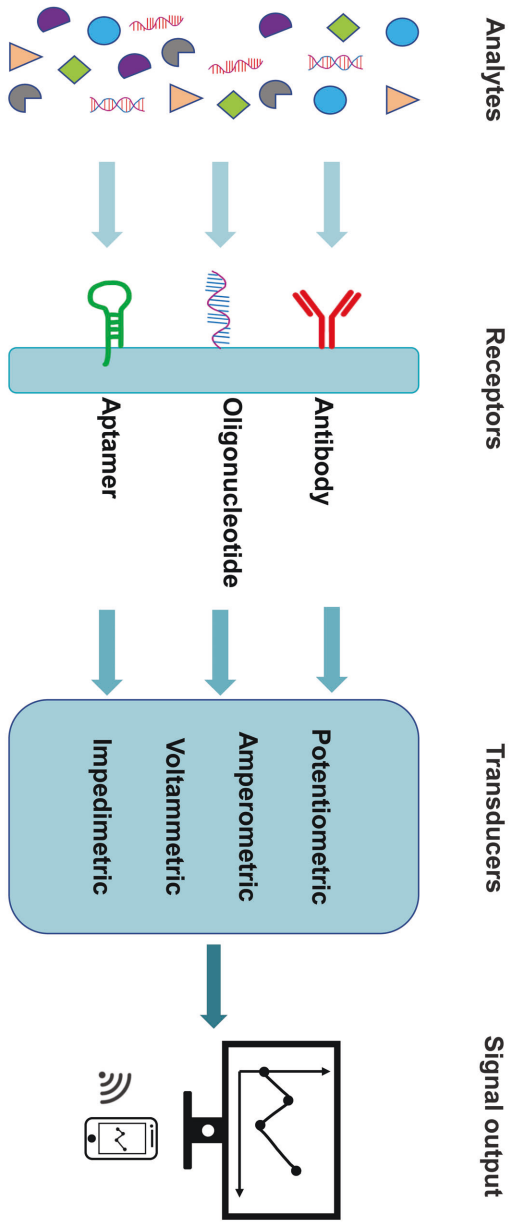

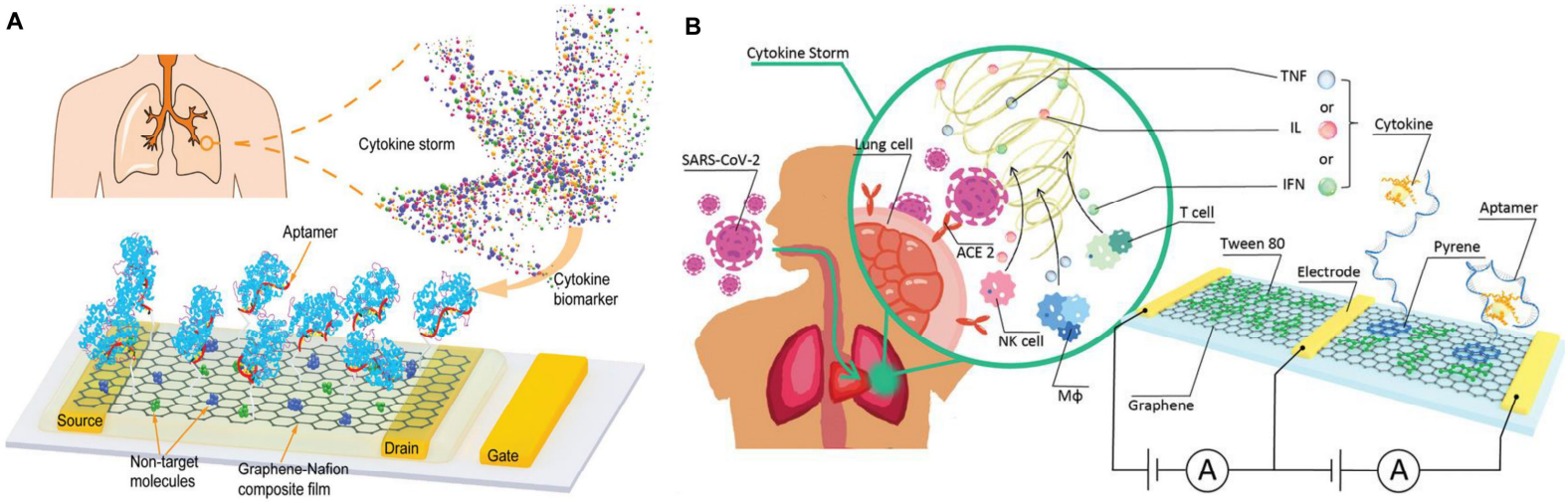

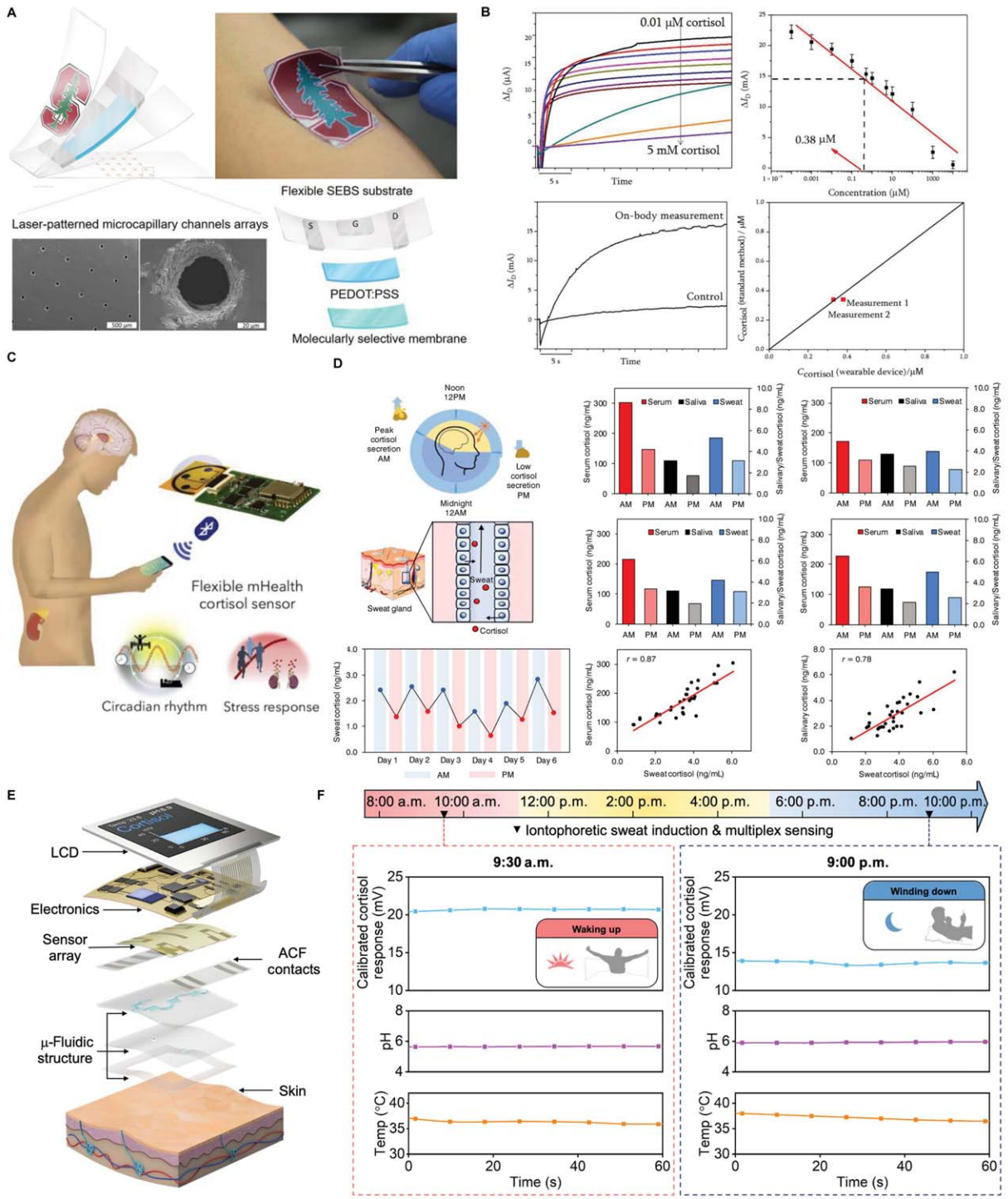

PLEASE CITE THIS ARTICLE AS DOI: 10.1063/5.0140900

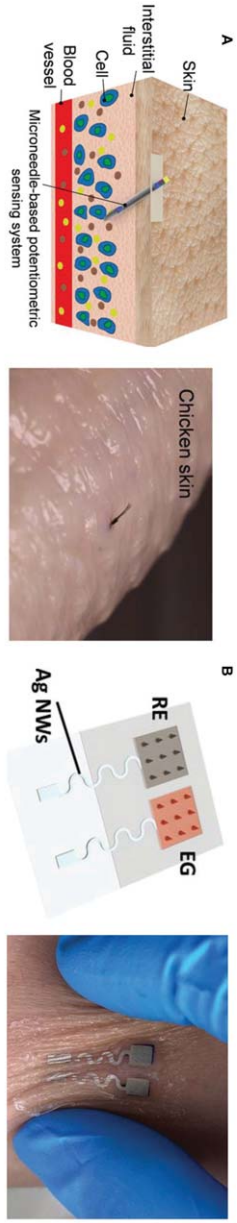

PLEASE CITE THIS ARTICLE AS DOI: 10.1063/5.0140900

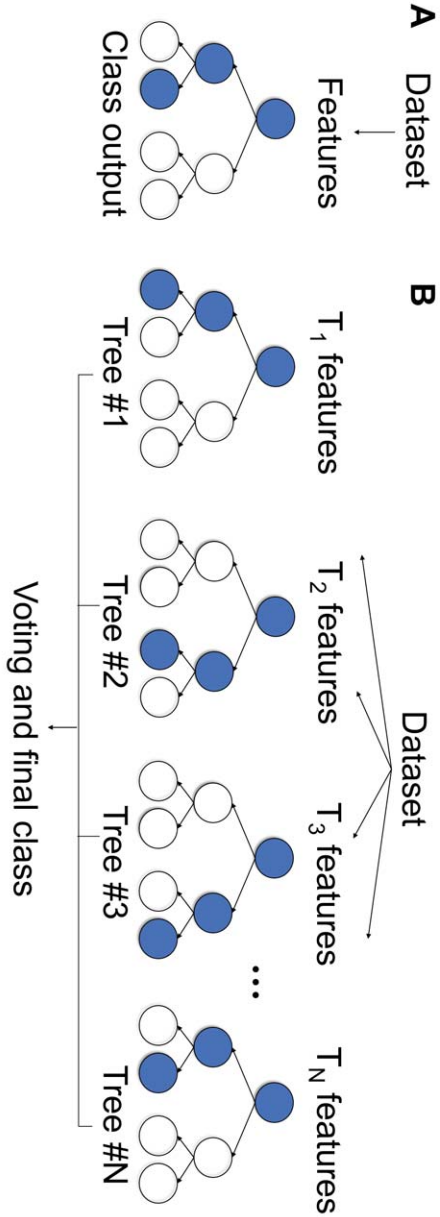

PLEASE CITE THIS ARTICLE AS DOI: 10.1063/5.0140900